





This is to certify that the

dissertation entitled

OBSERVATION OF NEURAL ACTIVITY AS A VARIATION OF MICROWAVE IMPEDANCE

presented by

Trygve Gene Aaby

has been accepted towards fulfillment of the requirements for

PhD degree in Biophysics

Date Aug. 27,1982

MSU is an Affirmative Action/Equal Opportunity Institution

0-12771



RETURNING MATERIALS:
Place in book drop to
remove this checkout from
your record. FINES will
be charged if book is
returned after the date
stamped below.

ACT CT 36 ::

OBSERVATION OF NEURAL ACTIVITY AS A VARIATION OF MICROWAVE IMPEDANCE

Ву

Trygve Gene Aaby

A DISSERTATION

Submitted to
Michigan State University
in partial fulfillment of the requirements
for the degree of

DOCTOR OF PHILOSOPHY

Department of Biophysics

1982

Copyright by
TRYGVE GENE AABY
1982

ABSTRACT

OBSERVATION OF NEURAL ACTIVITY AS A VARIATION OF MICROWAVE IMPEDANCE

Βy

Trygve Gene Aaby

Evidence is presented that neural tissue can exhibit spatial and temporal variations of its microwave impedance provided that the microwave probe field is properly coupled to the tissue. Such coupling is achieved by applying a 10 GHz evanescent field of less than one cubic millimeter extent to the ventral nerve cord of the cockroach <u>P. americana</u>. The experimental apparatus consisted of a variant of a standing wave tube in which a section of coaxial cable functioned simultaneously as a probe of microwave impedance and of the volume conducted fields within the tissue.

Recordings are presented which show the simultaneous changes in the microwave impedance and in the electrical activity of the tissue. Similarities in the waveforms of these two signals can be observed, and the two signals appear strikingly similar when the electrical signal is passed through a low-pass filter. These signals appear not to be caused by muscular activity but often appear to occur in association with faintly visible microscopic deformations of the surface of the cord. The inertia of the tissue appears to limit the impedance changes to frequencies of less than 10 Hz.

Evidence is presented that this phenomenon is electromechanical in nature, being due fundamentally to structural
alterations of the electrical double layers surrounding the
cellular membranes. The microwave impedance technique is
shown to be useful in detecting changes in the density of
action potentials, and this technique has the additional
feature of not requiring direct contact of an electrode with
the tissue under investigation.

This thesis is dedicated to the late

Department of Biophysics,

Michigan State University (1962-1982),

and to the living spirit of rock n' roll.

ACKNOWLEDGMENTS

The author wishes to thank all those who contributed to this work, in particular: Dr. Barnett Rosenberg, who provided work space, materials, funding, and constant support of this and several related projects; Dr. Gabor Kemeny, whose critical efforts led to many improvements in equipment, methods, and understanding of results; Dr. Bela Karvaly, who was always quick to help out: Mr. Haislip Hayes, who acted over the duration of this project as a brother and friend and willingly offered the use of his critical eyes and agile hands to the progress of this project; Mr. Sid Wiener, who helped sustain the author in several particularly bleak moments; and Mr. Jeff Scott, who as a former member of Dr. Matsamura's laboratory provided an abundant supply of cockroaches. The author is also deeply indebted to his wife, Ms. Rose McConnell, who put up with his frequent mania and tried to keep the image of the light at the end of the tunnel burning brightly. Finally, the author wishes to express gratitude to his father and friend, Dr. Gene Aaby, who acted as a benefactor and mentor during the course of this project and was instrumental in helping to keep the dogs at bay.

TABLE OF CONTENTS

LIST OF	FIGURES	νi
Chapter		
1	INTRODUCTION	1
2	DISCUSSION OF THE EXPERIMENTS	22
3	DISCUSSION OF THE RESULTS	45
4	SUMMARY AND CONCLUSIONS	65
Appendi>	<u> </u>	
Α	SCHEMATIC DIAGRAMS FOR THE EMT	70
В	BASIC ELECTRICAL STRUCTURE OF INTERFACES	76
С	AN ELECTROMAGNETIC FORMALISM PERTINENT TO	
	THE ANALYSIS OF MEDIA BY MICROWAVE REFLECTANCE	81
D	MICROWAVE REFLECTANCE FROM OHMIC MEDIA	91
Ε	MICROWAVE REFLECTANCE FROM NON-OHMIC MEDIA	95
REFERENC	CFS	109

TABLE OF CONTENTS

LIST OF	FIGURES	v i
Chapter		
1	INTRODUCTION	1
2	DISCUSSION OF THE EXPERIMENTS	22
3	DISCUSSION OF THE RESULTS	45
4	SUMMARY AND CONCLUSIONS	65
Appendi	<u>x</u>	
Α	SCHEMATIC DIAGRAMS FOR THE EMT	70
В	BASIC ELECTRICAL STRUCTURE OF INTERFACES	76
С	AN ELECTROMAGNETIC FORMALISM PERTINENT TO	
	THE ANALYSIS OF MEDIA BY MICROWAVE REFLECTANCE	81
D	MICROWAVE REFLECTANCE FROM OHMIC MEDIA	91
Ε	MICROWAVE REFLECTANCE FROM NON-OHMIC MEDIA	95
REFEREN	CES	109

LIST OF FIGURES

Figure		
1	Illustration of Resonance Perturbation	7
2	A Standing Wave Tube (SWT) Viewed in Cross-Section	8
3	A Block Diagram of the Electromagnetrode (EMT)	1 1
4	A Method for Locating the Effective Boundary of the EMT Probe Field	12
5	A Method for Demonstrating That the Probe Field Is Not Perturbed by Electrolysis in Bulk Phase	14
6	A Method for Demonstrating That the Probe Field May Be Perturbed by an Electrified Interface	15
7	A Method for Demonstrating That the Probe Field May Be Perturbed by Plasma Oscillations	17
8	A Sketch of the Method for Recording Vari- ations of Electrical Potential and Microwave Reflectance Associated with the Activity of the Cockroach Nerve Cord (VNC)	20
9	Microwave Impedance Changes Produced by Electrical Stimulation of the Cockroach Nerve Cord	23
10	DC Recording of the Microwave Impedance Changes Produced by Electrical Stimulation	27
11	DC Recording of the Microwave Impedance Changes Produced by Electrical Stimulation, continued	28
12	Spontaneous Activity of the Cockroach Nerve	32

13	A 2x Magnification of Figure 12	33
14	A Comparison of the Raw and Filtered EL Signals with the MW Signal	34
15	A Comparison of Regular and Irregular Phases of Spontaneous Activity	35
16	A Recording Exhibiting Good Correlation Between the MW and the MEL Signals	37
17	A 2x Enlargement of Figure 16	38
18	A Comparison of MW, Raw EL, and Filtered EL Signals	39
19	Typical EMT Signals	41
20	Typical EMT Signals	42
21	Typical EMT Signals	43
22	EMT Signals Obtained with No Visible Activity of the Tissue	58
23	Responses to Stimulation of the Cerci with No Visible Motion of the Nerve Cord	59
24	Typical EMT Signals with No Visible Motion of the Nerve Cord	60
A – 1	Schematic Diagram of EMT Power Supply	71
A - 2	Connections from Power Supply to the Amplifiers	72
A-3	Connections from Power Supply to the Gunn Diode	73
A - 4	Schematic Diagram of the EMT Physiological Amplifier Circuit	74
A - 5	Schematic Diagram of the Standing Wave Tube Amplifier of the EMT	75
B - 1	An Illustration of Electric Field and Charge Distribution at the Interface	80
C - 1	Complex Field Configurations in K ,ω Space	87

CHAPTER 1

INTRODUCTION

The fundamental hypothesis underlying the work described in this thesis is that the physiological activity of neural tissue may appear as a spatially and temporally variable impedance with respect to an impressed electromagnetic field oscillating at gigahertz frequencies. Such an applied field, called the probe field (PF), will then be temporally modulated by the neural activity, and the spatial extent of the probe field will determine the total volume of the tissue over which the physiological activity is being monitored. Consequently, information about the physical processes which comprise the neural activity of the tissue can be gained by investigating the modulation of the probe field.

In a general sense, this kind of investigation has been carried out many times before, and several investigators have reported modulation by neural activity using probe fields of various frequencies. In 1939, K. S. Cole and H. J. Curtis [1] presented the classic measurements of changes in the impedance of the squid giant axon which occur when the action potential is initiated. These investigators limited the applied frequencies to the

kilohertz region of the electromagnetic spectrum. In practice, a segment of squid axon was used as one arm of a balanced Wheatstone bridge; activity of the nerve was observed to throw the bridge out of balance in a quantitative manner. These experiments are now described in basic textbooks of neurophysiology [2, 3], because they led to the recognition that the conductance of the axon membrane is the principal parameter involved in excitability, so that the kilohertz impedance studies paved the way to the development of the voltage-clamp technique.

A similar technique of monitoring changes in the kilohertz impedance due to neural activity has also been used in studies of brain function, notably by W. R. Adey, R. T. Kado, et al., and by J. B. Ranck, Jr. These investigators and their colleagues have studied the effects of paradoxical sleep, anesthesia, and spontaneous activity upon the kilohertz impedance of local regions of the brains of several mammalian species [4, 5]. Van Harreveld, et al., have utilized a kilohertz impedance technique as a means for studying seizure activity and spreading cortical depression in the rabbit [6]. In general, kilohertz impedance studies of brain tissue appear less easy to interpret than do studies of squid axon or peripheral nerve. The impedance variations are less consistent in waveform, and correlations between physiological activity and the observed impedance changes are more difficult to establish. Consequently, these results are discussed in terms of

percentage shifts of impedance, and the impedance recordings are displayed in the time domain as raw data for comparison with simultaneous EEG recordings. Often the results are of a statistical nature, with only a sample of the total number of tested animals showing a definite response to a given stimulus. Nevertheless, kilohertz impedance techniques are a useful addition to neurophysiological research, and W. R. Adey has suggested [5] that impedance studies might profitably be extended into the microwave, infrared, and visible frequency regimes.

A sizeable literature exists describing changes in the optical impedance of nerves when the action potential is initiated [7-9]. In particular, L. B. Cohen, B. Hille, and R. D. Keynes have shown [7] that in the crab leg nerve, a definite optical retardation (i.e., change in the birefringence) accompanies the action potential, with a magnitude of about one part in ten thousand. This birefrigence change appears to be localized to the membrane, although other investigators [8] find that the birefringence is not due to the direct action of the trans-membrane electric field upon the membrane lipids but rather to a complex process involving lipid-soluble ions in the membrane. Even though optical impedance techniques are difficult to exploit, they do provide information about ion carriers in the axonal membrane.

It is primarily because impedance changes reflect structural changes that investigators continue to explore

the impedance properties of active neural tissue at various frequencies. In a comprehensive review article [9], L. B. Cohen describes a wide range of techniques useful in the investigation of structural changes occurring during action potential propagation and synaptic transmission. Among these is the study by M. H. Sherebrin, et al. [10] in which olfactory nerves of the garfish, frog sciatic nerves, and nerves of the walking legs of lobsters were observed to exhibit differential absorbance in the infrared when stimu-In particular, the differential absorbance appeared lated. to be due to alterations in the frequency of the P-O-C stretch (1030 cm^{-1}). Consequently, alterations of the membrane conformation as a result of excitation appear to comprise the structural changes which are manifested in the infrared impedance changes.

The studies mentioned above show that the changes in the impedance of neural tissue with activity are discernable over wide ranges of applied frequency (e.g., kilohertz, infrared, and visible), and it is somewhat natural, then, to inquire as to the possibility of observing neural activity as a variation of microwave impedance. In fact, a large literature exists which describes the steady-state impedance of various tissues at megahertz and gigahertz frequencies [11, 12]. These studies have been carried out primarily to assess the physiological effects of microwave radiation, although the analysis of the reported effects remains ambiguous [13-15]. In general, it appears that

microwave impedance measurements are more difficult to obtain quantitatively than impedance measurements at kilohertz or optical frequencies, and this seems to be due principally to the fact that kilohertz wavelengths are so long that ordinary lumped-circuit theory applies, while at optical frequencies, the wavelengths are so short that the principles of geometrical optics obtain. At microwave frequencies, the wavelengths are on the order of centimeters so that complicated interference effects arise in most experiments. Furthermore, the technology required for microwave impedance measurements can be quite cumbersome, involving the use of waveguides, klystrons, and directional couplers.

In 1963, J. B. Gunn announced the discovery that appropriately manufactured crystals of gallium arsenide will emit continuous microwave radiation when properly biased [16]. Since that time, microwave sources have become available at low cost so that the design of monitors of microwave impedance for biophysical experimentation has become feasible. Several such monitoring devices have been constructed to date [17] for the purpose of observing microwave impedance changes associated with the cardiac and neural activities of animals. The proper subject of this thesis begins, then, with a description of the experimental means by which microwave impedance changes of active neural tissue can be detected.

The basic physical phenomenon which is utilized in the investigations described below is called resonance perturbation and is illustrated in Figure 1. A Gunn diode (G) is biased so that a microwave field appears at a radiating aperture in the Gunn diode housing. This field, called the source field, irradiates both a detector diode (D) and a quarter-wave antenna (A). The quarter-wave antenna is coupled to an appropriate length of coaxial cable (C), the distal end of which is truncated with a short length of exposed center conductor. Experiment readily shows that the fields at each end of the coaxial cable are in resonance, i.e., the source field and the probe field exhibit a definite reciprocity. If the probe field is undisturbed, the detector diode yields a steady voltage, known as the offset voltage, which is due to its presence in the source field. The relative positions of the antenna probe, the source field, and the detector diode influence the magnitude of the offset voltage, but if these are fixed, then the offset voltage becomes a function of the probe field configuration alone. The probe field may be perturbed by altering the dielectric constant of the medium in which the probe field is established. As a crude example, touching the probe tip with a finger may alter the offset voltage by as much as twenty percent.

In practice, the arrangement shown in Figure 1 is replaced by that of Figure 2. The source field is confined to the interior of a cylindrical cavity, and this serves to

Figure 1. Illustration of Resonance Perturbation.

By applying proper bias (+VDC) to the Gunn diode (G), a source field of microwave energy is generated. This field has a power density of 10 mW/cm² and a frequency of 10 gigahertz (X-band). An offset voltage appears across the leads of a microwave detector diode (D) placed in the source field; this voltage can be referred to ground and amplified to yield a signal output. A quarter-wave antenna (A) is also located in the source field; its location has a great effect upon the magnitude of the offset voltage. The antenna is connected to a length of coaxial cable (C) which conducts microwave energy away from the source field to form a probe field (PF) at the free end of the cable. The probe field and the source field exhibit a certain reciprocity such that perturbation of the probe field will yield a variation of the offset voltage.

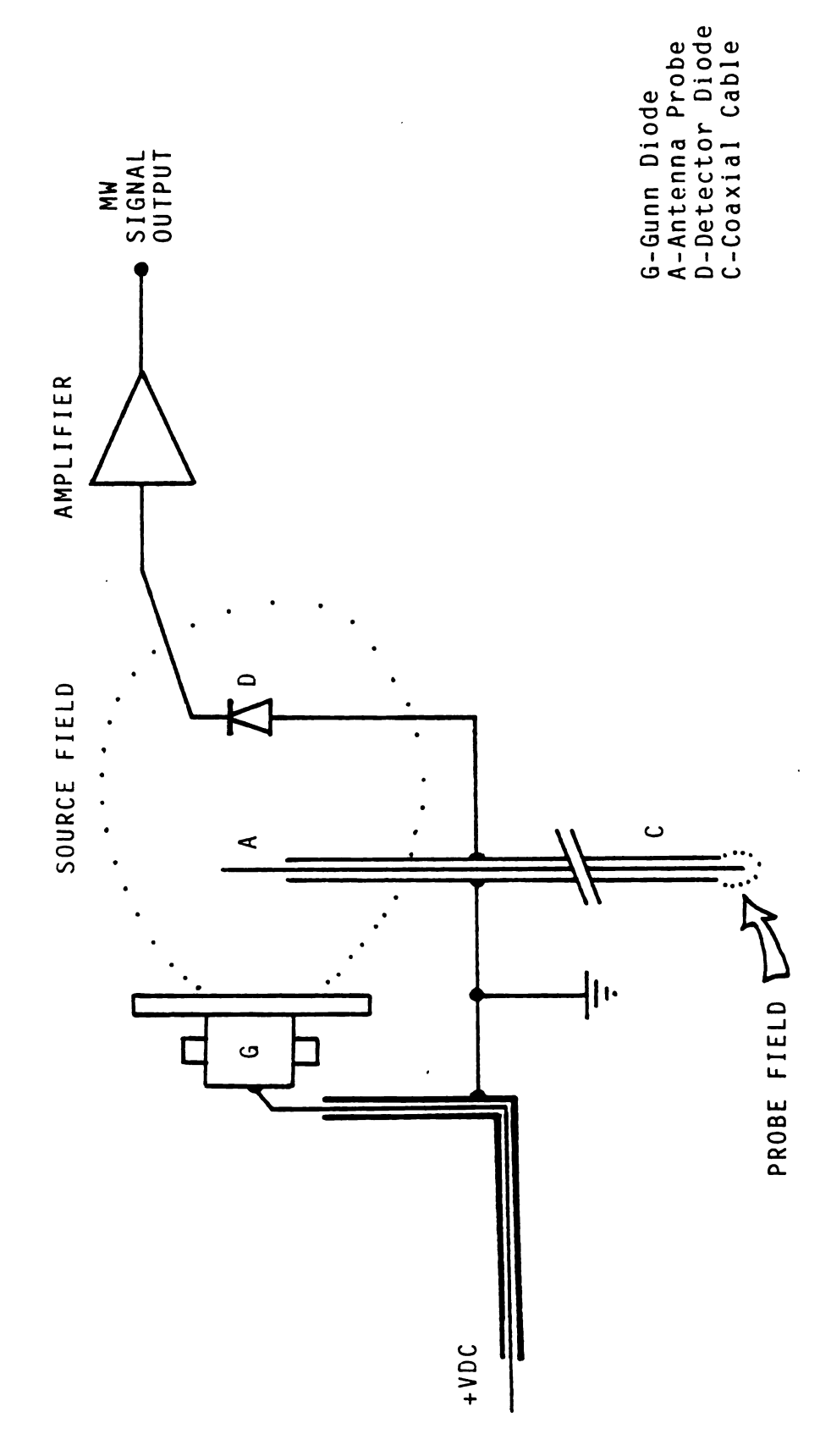
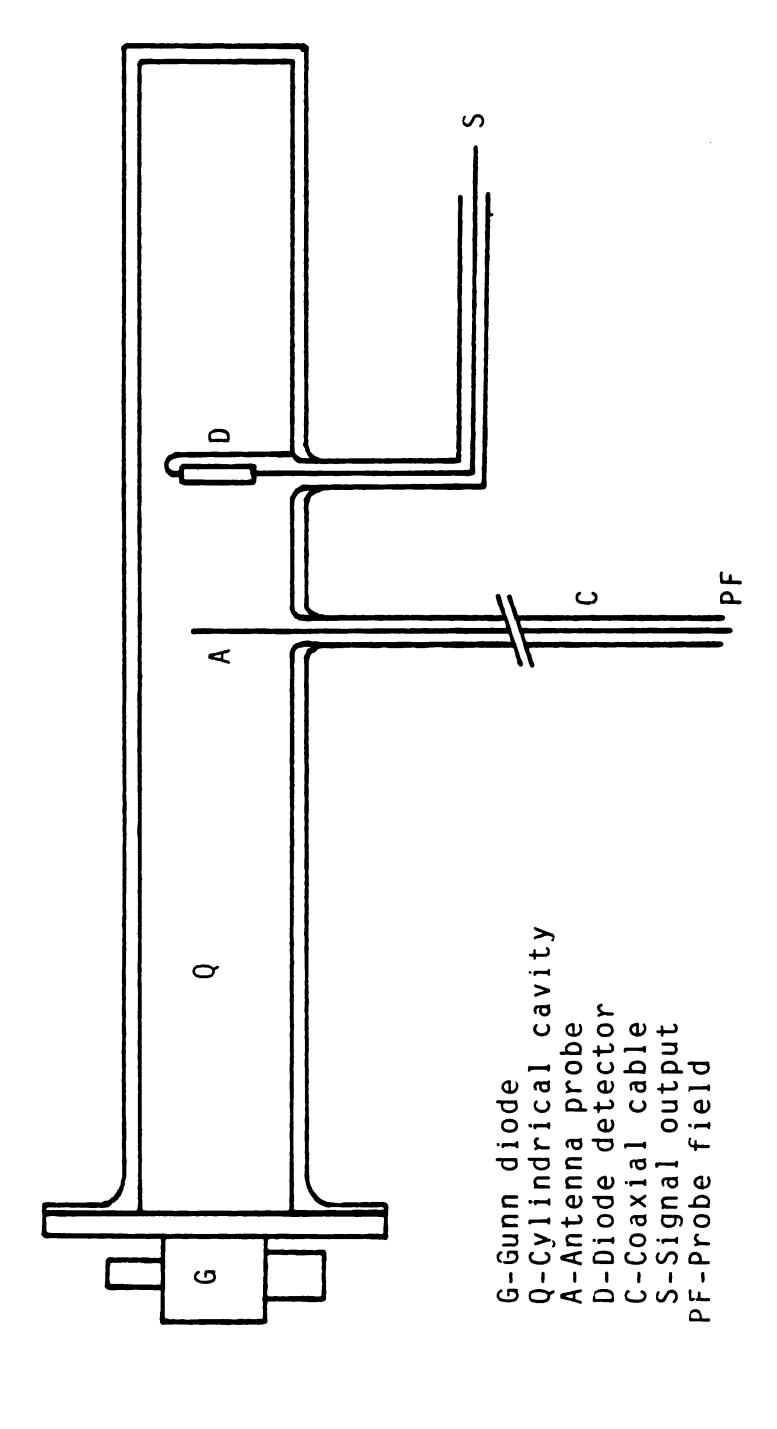


Figure 1. Illustration of Resonance Perturbation.



A Standing Wave Tube (SWT) Viewed in Cross-Section. Figure 2.

contain the source field so that experiments may be conducted without introducing extraneous modulation of the microwave field. The microwave field must be enclosed tightly within the cavity, otherwise microwave leaks will be found to introduce spurious artifacts as experimenters move about in the vicinity of the apparatus.

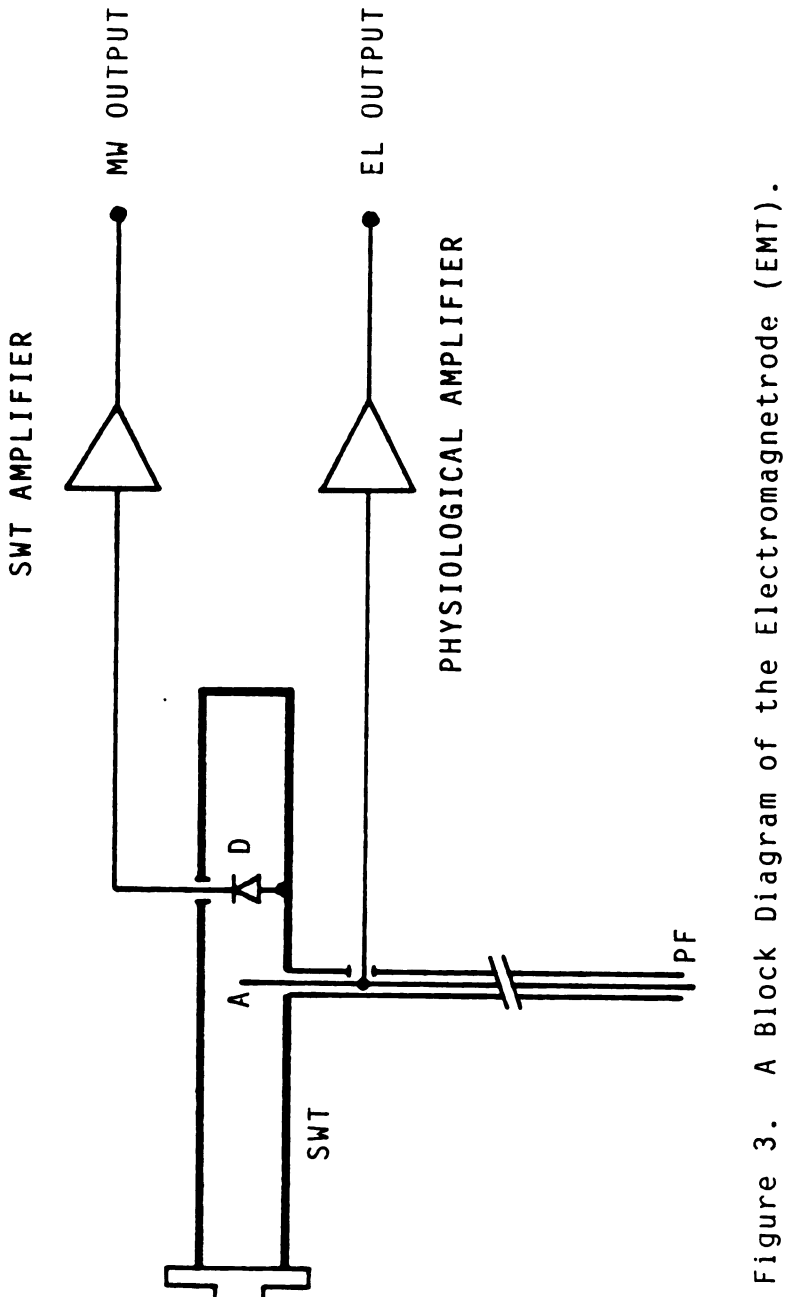
The cylindrical cavity shown in Figure 2 has the additional purpose of confining the source field to a configuration wherein only the lowest order modes are present. Thus, in practice, it is found that the microwave pattern inside the cylindrical cavity consists of an approximately monochromatic standing wave pattern. Naturally, the standing wave pattern is not ideal (as described in basic textbooks), due to the presence of the antenna probe and diode detector which act as scattering centers. Nonetheless, the device depicted in Figure 2 is called a standing wave tube (SWT) and is usable as a means for detecting changes in the microwave impedance of various systems [17]. Although the microwave field inside the SWT is not an ideal standing wave pattern, it is certainly more ideal than the source field depicted in Figure 1. Even so, the SWT is not as yet a calibrated instrument; the SWT is utilized in the work described below as a means to detect only relative changes in the microwave impedance of systems of interest.

The purpose of the present thesis is to provide evidence that the microwave impedance of neural tissue is altered as a result of neural activity. This evidence was

gathered by using a variant of the SWT, shown in Figure 3. This device, called the electromagnetrode (EMT), is simply a SWT which has a coaxial cable serving the dual purpose of establishing a microwave probe field and of detecting changes in the electrical potential occurring between the central and outer conductors exposed at the end of the cable. Thus, the EMT allows simultaneous detection of variations of electrical potential (EL) and microwave impedance (MW) occurring in a volume of tissue in the neighborhood of the probe tip of the coaxial cable. It should be noted that the central conductor of the coaxial cable which enters the SWT as a quarter-wave antenna is completely insulated from ground so that the electrical resistance between the inner and outer conductors is in excess of several megohms. Consequently, the application of the EMT to biological tissue is expected to load the tissue only nealiaibly.

Figure 4 illustrates a basic feature of the EMT probe, which is that the microwave and electrical potential signals are not mixed by the EMT. A dissection needle may be used to locate the effective boundaries of the microwave probe field (PF), since tiny motions of the needle act to perturb the microwave resonance. The electrical potential is not influenced by the presence of the needle unless the needle electrically contacts the central conductor of the probe tip.

A Block Diagram of the Electromagnetrode (EMT). က Figure A standing wave tube (SWT) is shown in cross section at the left; the offset voltage of the microwave detector diode (D) is amplified to yield the microwave output signal. The probe field (PF) produces a variation of the microwave output signal. The coaxial cable of the SWT has been modified so that electrical potential differences appearing near the probe can be amplified and recorded. This arrangement allows simultaneous monitoring of changes in the microwave impedance and electrical potential occurring in small samples, and the two output signals are independent of each other. Thus, whenever the two signals exhibit similar features, it is certain that both the microwave impedance and the electrical potential of the sample have varied in a similar



A Block Diagram of the Electromagnetrode (EMI).

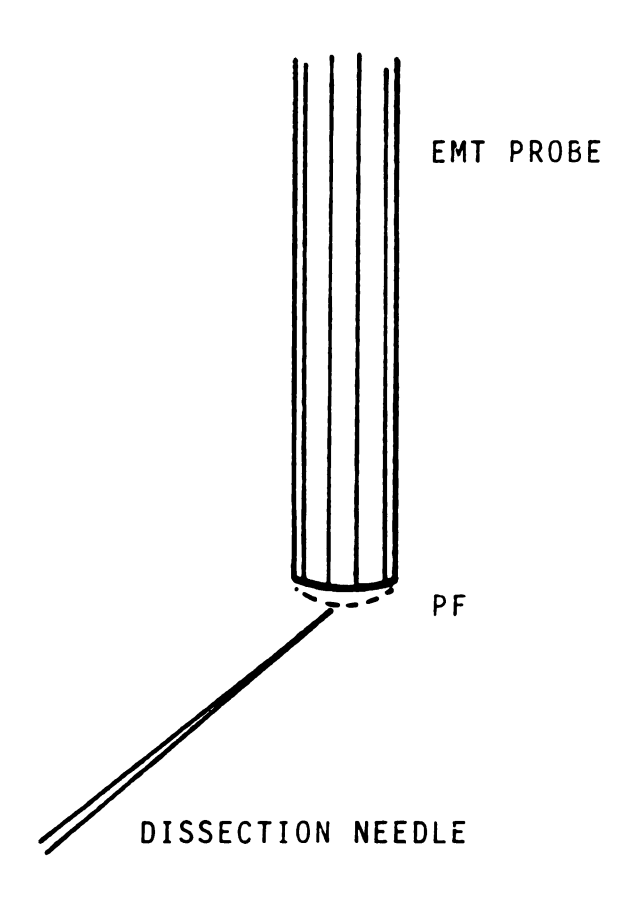


Figure 4. A Method for Locating the Effective Boundary of the EMT Probe Field.

The EMT simultaneously detects changes in the microwave impedance and the electrical potential of samples placed in the probe field. These two signals are not at all mixed in the EMT, as can be demonstrated by perturbing the probe field while not touching the tip of the coaxial cable.

A second basic feature of the EMT probe is illustrated in Figure 5. If the EMT probe is immersed into any liquid and a voltage is applied externally, no perturbation of the microwave impedance is observed, whereas a variation of the electrical potential is easily observed even for microvolts of applied signal. The impedance of bulk-phase media is wholly insensitive to variation by passage of electrical current so that it is certain that the microwave impedance of neural tissue will never vary because of stimulus artifacts or volume conducted fields, whereas these will be readily exhibited in the variation of electrical potential.

By contrast, the microwave impedance of an interface lying within the probe field can be altered by the application of an external electric field. As illustrated in Figure 6, the saline/mineral oil interface can yield microwave impedance changes when electrified by means of a signal generator. If an alternating voltage of low frequency (less than 10 Hz) is applied across the interface, a microwave signal can be detected which appears as a rectified version of the applied voltage. Application of a few volts peak-to-peak shows that the interface is distorted slightly but only for half of the cycle during which the voltage is applied. If the applied signal is reduced in magnitude, the periodic distortion of the interface becomes unobservable visually, with changes in the microwave impedance still readily detectable. Because of the inertia of the interface, the microwave impedance change will not follow the

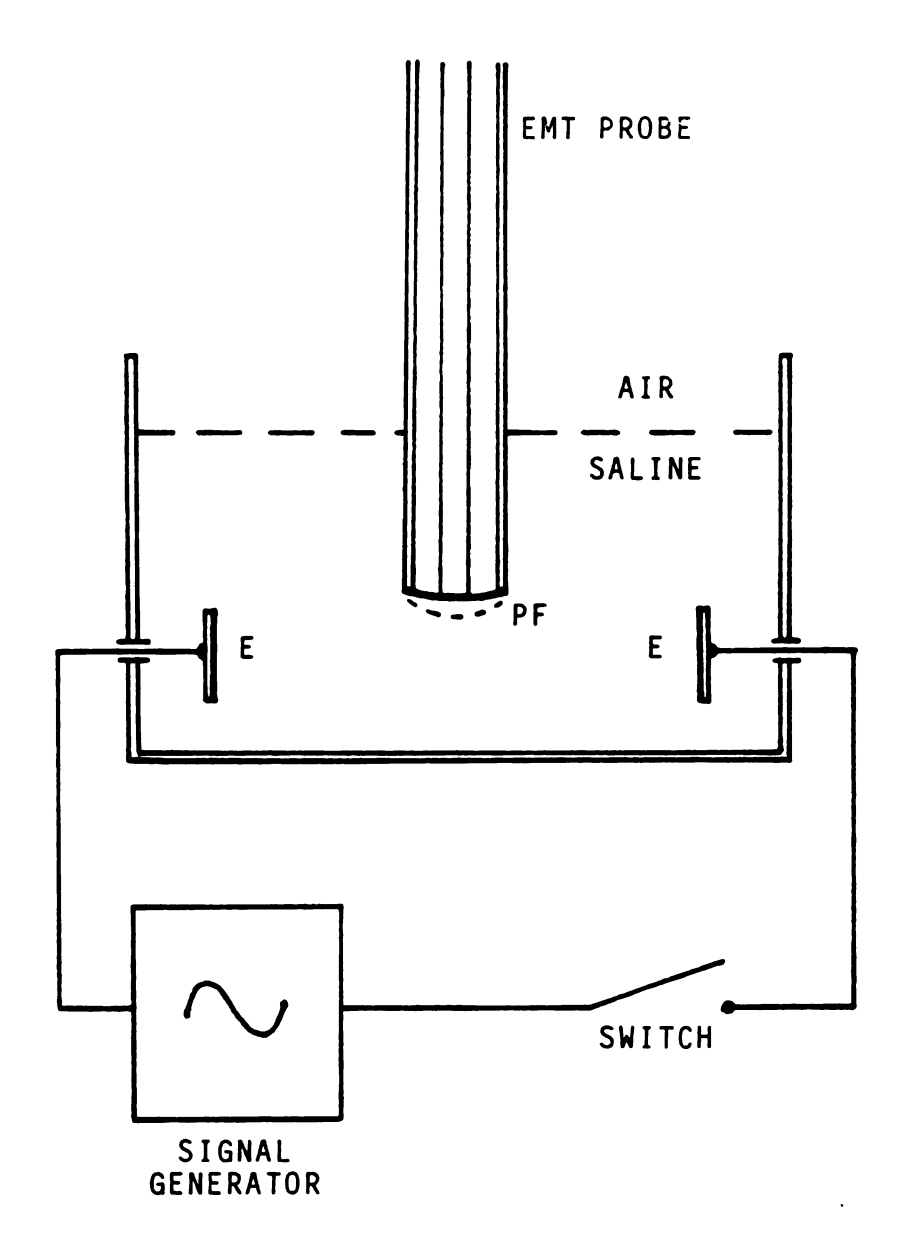


Figure 5. A Method for Demonstrating That the Probe Field Is Not Perturbed by Electrolysis in Bulk Phase.

The microwave impedance of bulk-phase media cannot be caused to vary by application of an external voltage. This is true for solutions of electrolytes as well as for organic liquids. Consequently, it is certain that simulus artifacts and volume-conducted fields will not generally be detectable as microwave impedance changes.

Figure 6. A Method for Demonstrating That the Probe Field May Be Perturbed by an Electrified Interface.

The microwave impedance of certain interfacial systems can be varied by application of an external voltage. One such system is the saline/mineral oil interface, which is distorted in a subtle fashion by the application of a few volts across it. This distortion yields an altered microwave impedance, which is readily detectable using the EMT. The interface exhibits rectification in that the distortion occurs during only half of the cycle of an applied alternating voltage. The inertia of the interface constrains the impedance variations to frequencies of less than about ten cycles per second. Application of frequencies higher than this produces a steady distortion, which varies only when the voltage is changed slowly in amplitude or frequency.

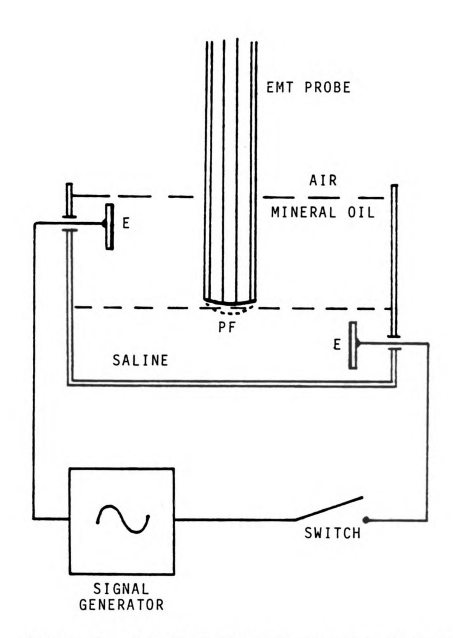


Figure 6. A Method for Demonstrating That the Probe Field May Be Perturbed by an Electrified Interface.

applied frequency above about 10 Hz. Application of frequencies higher than this produces a steady distortion of the interface which varies only when the voltage is changed slowly in amplitude or frequency. Consequently, the saline/mineral oil interface provides microwave impedance changes which are always slowly varying (i.e., 0 Hz to 10 Hz). A pulse of applied voltage elicits a response which rises and falls exponentially with a time constant of a few seconds in magnitude depending on the total area of the interface. Pulse trains with repetition rates of a few pulses per second will cause the individual responses to summate exponentially.

Rapidly varying microwave impedance changes can be produced by a method illustrated in Figure 7. The plasma oscillations within a neon light bulb are readily detectable as changes of microwave impedance. When the plasma is driven by frequencies as high as 20 KHz, the microwave impedance changes can be observed easily on an oscilloscope, and the applied signal and the microwave response are then seen to possess the same frequency. This result shows that the frequency response of the EMT extends into the kilohertz range. Of course, at these frequencies the plasma appears motionless to the eye. As is well known [18], the ionized gas within the bulb undergoes density variations in response to the applied voltage. Also, it is the plasma density which is responsible for determining the magnitude of the microwave impedance. Consequently, the

Figure 7. A Method for Demonstrating that the Probe Field May Be Perturbed by Plasma Oscillations.

Alternating current with a peak-to-peak voltage of about fifty volts can be used to ignite a neon bulb, which glows in the region of the ionized gas. The ionized gas has a density in the neighborhood of 10 10 Using basic physics, it can be shown that the natural frequency of plasma oscillations for a plasma of this density is in the gigahertz range. These oscillations are of the longitudinal type, and no microwave radiation is produced, as can be readily demonstrated by placing a microwave detector diode near the illuminated bulb. The plasma acts as a medium which has a large microwave impedance, and this impedance is directly related to the plasma density through the plasma frequency. Because the plasma is driven by an alternating current, the plasma density varies at the same frequency. At kilohertz frequencies the plasma appears motionless to the eye, yet the EMT follows the oscillating microwave impedance easily. In this manner, it is shown that the frequency response of the EMT extends from zero cycles per second well into the kilohertz range.

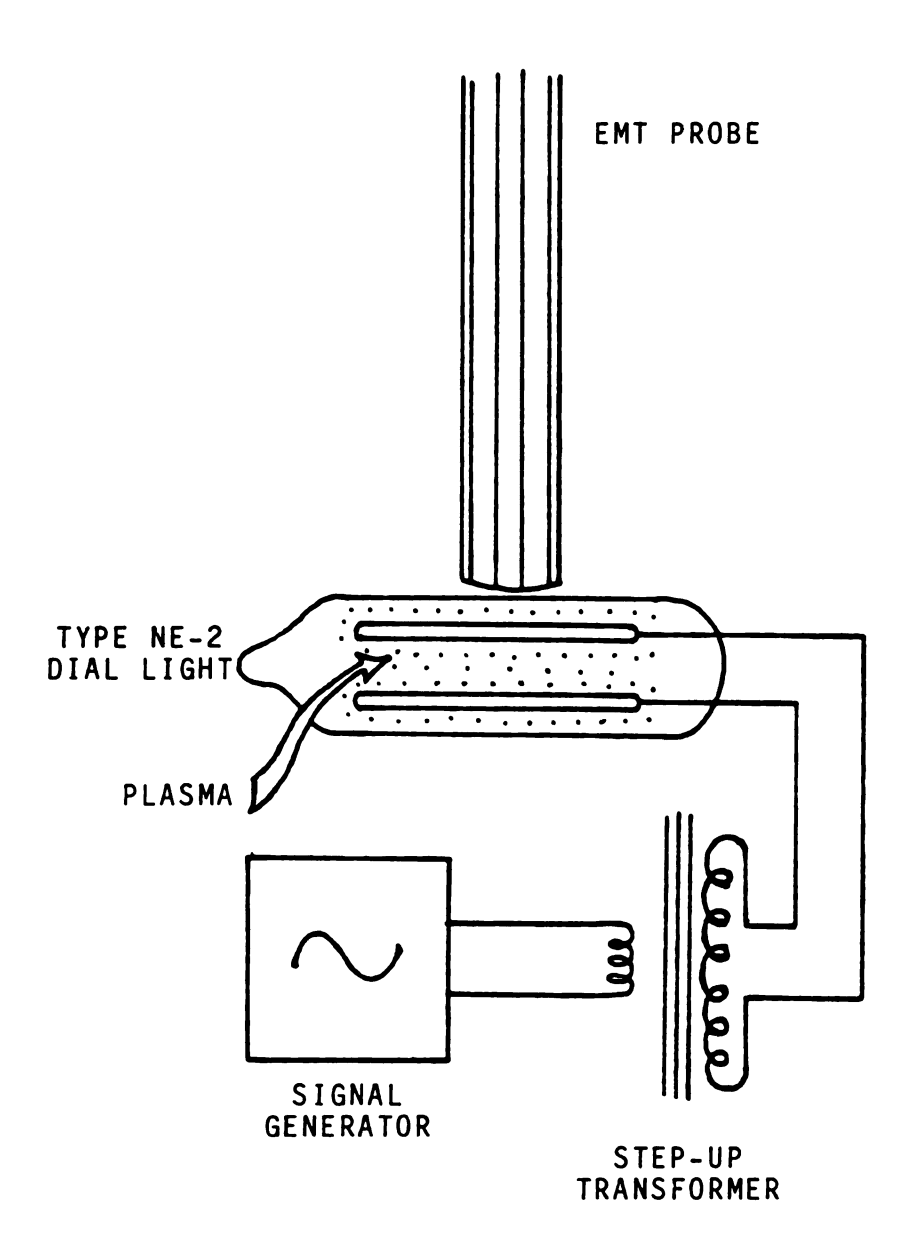


Figure 7. A Method for Demonstrating That the Probe Field May Be Perturbed by Plasma Oscillations.

applied signal varies the microwave impedance and thus modulates the microwave probe field.

Another interesting feature of the neon plasma is that it emits no detectable microwave radiation, as can be seen by placing a microwave detector diode next to the bulb and noting the absence of an offset voltage across its leads. This is noteworthy since it shows that a system need not emit microwave frequencies in order to possess a variable microwave inpedance. Furthermore, if the amplitude of the signal applied to the bulb is reduced, the modulation of the microwave probe field is also reduced, and the modulation ceases abruptly when the plasma is turned off. Raising the applied voltage from zero yields no modulation until breakdown is suddenly reached and the plasma is formed.

Figures 4-7 illustrate a number of fundamental facts about the EMT and the principles of its operation. For the sake of clarity, these can be listed as follows:

- (a) The two channels of the EMT, denoted MW and EL, are not mixed in the EMT. These signals represent changes in microwave impedance and electrical potential, respectively.
- (b) The frequency response of both the MW and the EL channel is known to extend from zero frequency will into the kilohertz region.
- (c) The bulk-phase microwave impedance of materials is not variable by the application of electric fields of

ordinary strength. Even using step-up transformers and studying a wide variety of liquids, no modulation of any bulk-phase material has yet been observed with the EMT.

- (d) Interfacial microwave impedance can be varied by the application of modest voltages (i.e., a few volts) in some systems. The saline/mineral oil interface is such a system, and structural changes at the interface can be seen to occur in association with the microwave impedance changes when the voltages are of sufficient magnitude.
- (e) Ionized gas of the proper density represents a system which exhibits a large microwave impedance, and this impedance can be readily modified by electrical means.

At this point, it is appropriate to consider Figure 8, which shows the EMT probe in a configuration suitable to detect simultaneously the changes in microwave impedance and electrical potential of neural tissue. The ventral nerve cord of the cockroach P. americana is shown surgically extirpated from the body wall and covered with physicological saline suitable for cockroach tissue [19]. Figure 8 shows the EMT probe and the nerve cord drawn approximately to scale as they would appear under the dissecting microscope. This is the basic configuration used to record all of the data presented below. In practice, the cockroach is pinned out on a wax block, and the EMT

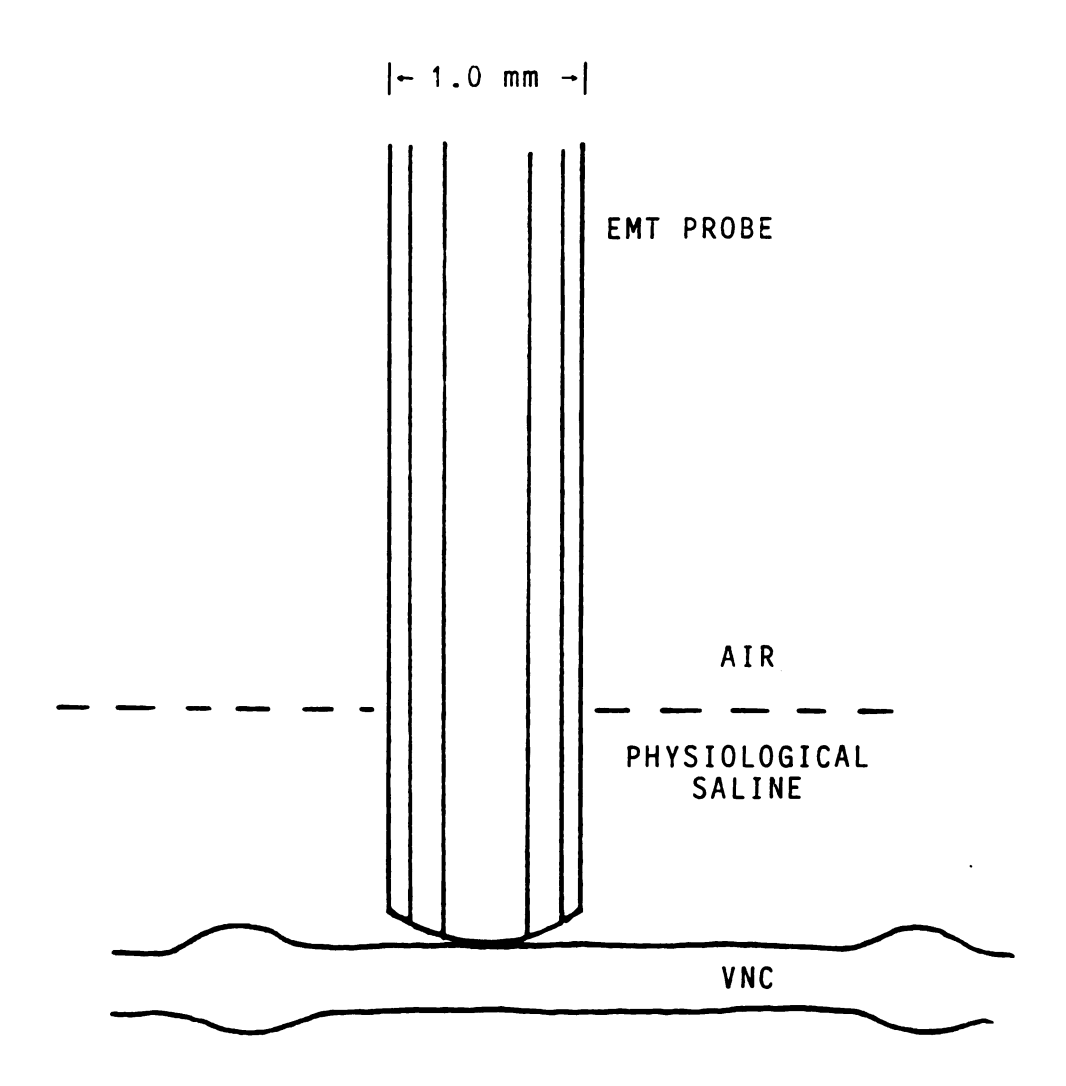


Figure 8. A Sketch of the Method for Recording Variations of Electrical Potential and Microwave Reflectance Associated with the Activity of the Cockroach Nerve Cord (VNC).

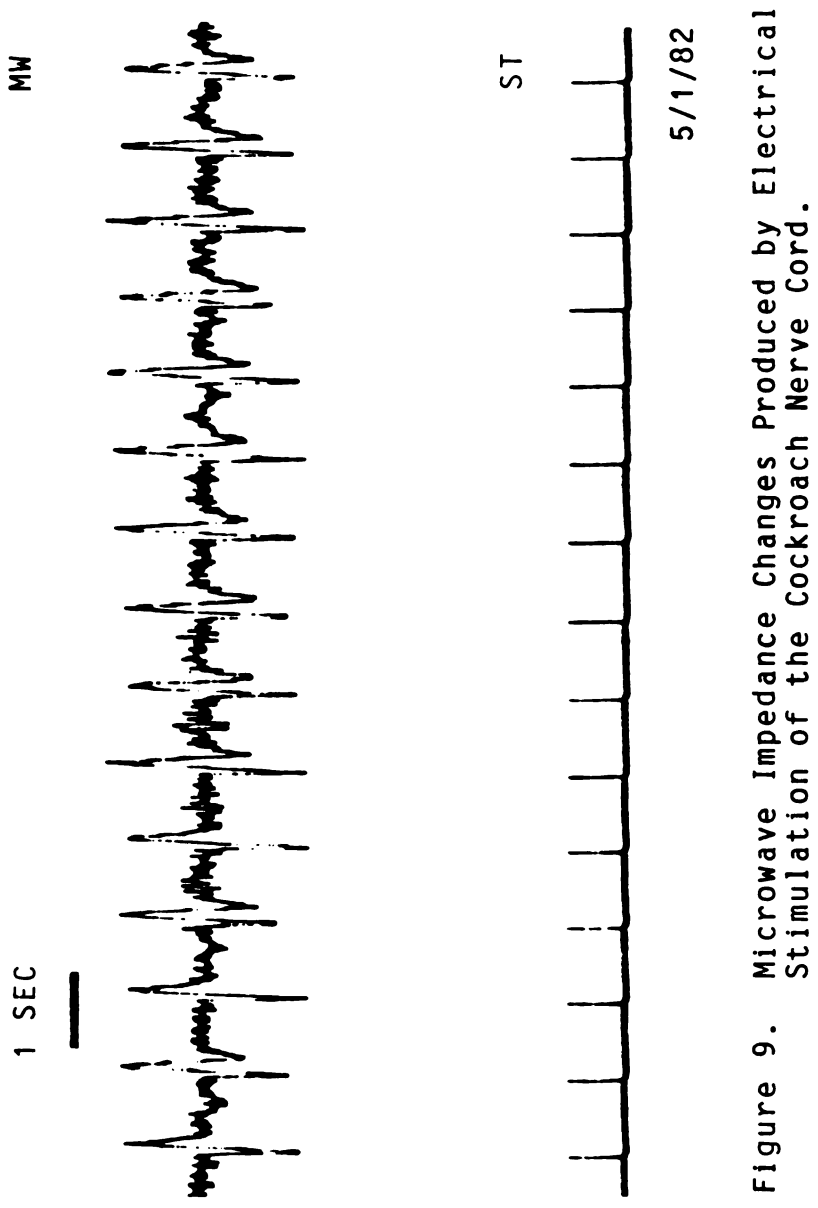
probe is held in position using a micromanipulator. Thus, this arrangement is similar to that used with conventional neurophysiological recording techniques. In principle, the arrangement is also not dissimilar to those used by investigators who have recorded impedance changes of neural tissue in the kilohertz, infrared, and optical regimes.

Having now considered the history of impedance techniques as applied to neurophysiological research and having discussed a means of extending the impedance technique into the microwave regime, it is now appropriate to present the results of experiments performed on cockroach nerve cord using the EMT. These results are presented in the next chapter.

CHAPTER 2 DISCUSSION OF THE EXPERIMENTS

Appendix A gives a complete technical description of the electronic circuitry incorporated into the EMT which was used in the present study. The electrical potential signal (EL) of the EMT was connected to one channel of a Tektronix 5113 Dual Beam sotrage oscilloscope, and the microwave impedance signal (MW) was connected to another channel. Thus, both signals could be observed simultaneously on the oscilloscope. Both signals were also connected to a Gilson 5/6 H Biophysical Recorder with IC-MP plug-in modules. The EL signal was also fed into an audio monitor consisting of a Kenwood KA 3700 amplifier and a loudspeaker. The purpose of these connections was to observe the microwave impedance changes and electrical potential variations of active neural tissue in as complete a manner as possible.

Figure 9 shows a record of the microwave impedance changes produced by electrical stimulation of the cockroach ventral nerve cord. The EL signal from the EMT has been omitted in this figure because the stimulus artifact swamps the electrical response of the tissue. In this experiment, cathodic voltage pulses of 10 msec duration and



approximately one volt in amplitude were delivered to the nerve cord with respect to the body wall. This was accomplished by using clean insect pins as electrodes, the pulses being delivered from a Grass stimulator and stimulus isolation unit. The pulses were delivered at a rate of one per second. The MW response for each stimulus pulse is clearly visible; the response consists of a biphasic excursion of approximately 0.2 seconds duration. The MW signal is clearly distinct from the baseline noise.

The duration of the response indicates that it is not due to the unit action potential, for in the cockroach, the spontaneous action potentials are only about one or two milliseconds in duration. The duration is not an artifact of the EMT amplifiers, as was shown by the method illustrated in Figure 7. Consequently, the duration of the response is problematical and must be ascribed to some process which varies more slowly than the unit action potential. One possibility is that the MW response is due to compound action potentials which have a broader envelope and longer duration than unit action potentials. Another possible explanation for the duration of the responses seen in Figure 9 is that the stimulation has caused the nerve cord to be slightly pulled, twisted, or in some way subtly distorted in form so that the long duration of the response is due to mechanical inertia as the nerve tissue relaxes.

Figure 9 illustrates a fundamental problem which has plagued the present work since its inception: definite MW

signals can be obtained from neural tissue, but the physical origin of these signals is unclear. The following viewpoint will be adopted through the present work: signals from neural tissue will be considered genuine when they can be seen to be due to any physiological process except the contraction of muscular elements attached to the tissue surrounding the nerve cord. This viewpoint then accepts electrical effects, chemical effects, thermal effects, and any mechanical expressions of these effects as possible mechanisms which could yield microwave impedance changes as a result of neural activity. However, any MW response which can be seen to be due to the contraction of adjacent muscle fibers must be discarded from further consideration. Thus, as long as a MW response from neural tissue can be seen to occur in the absence of muscle activity, the response is considered genuine. In practice, this is accomplished by visual inspection of the nerve cord, as illustrated in Figure 8. The key criterion is not whether any visible changes are seen in the vicinity of the nerve cord but whether muscular effects are visible. This is an important distinction, since a preparation viewed as in Figure 8 will always exhibit microscopic activity due to the diffusion and convection of particulate matter in the bathing solution or to chromatic variations of light reflected from the nerve cord or even to the vibration of the laboratory bench upon which the experiment is conducted. Near the limit of visual detectability, even a

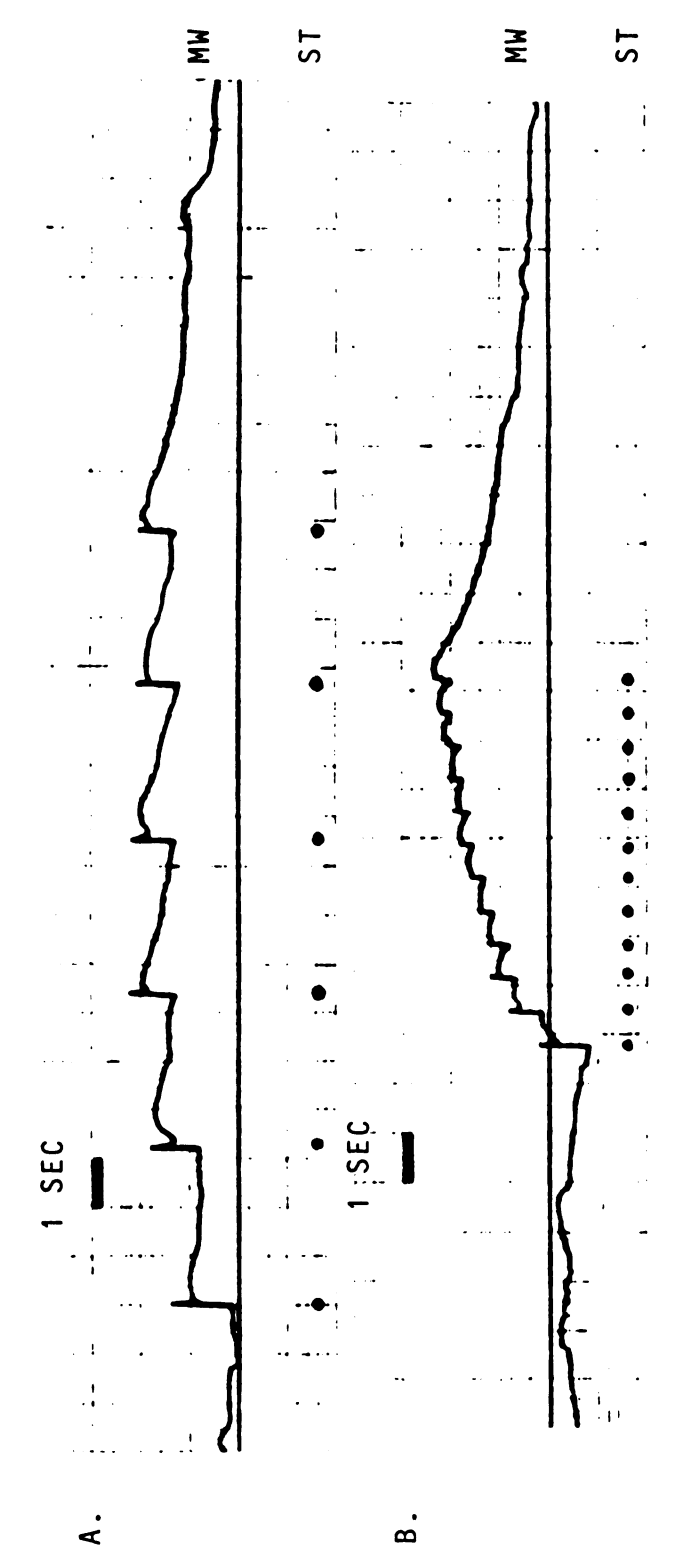
deceased preparation can exhibit a wealth of microscopic motions.

Consequently, it can be said of Figure 9 that although the MW response of the stimulated nerve cord may be due to a complex electromechanical process of some kind, it is apparently not due to muscular activity, and this indicates that the phenomenon is due to processes occurring within the neural tissue. This deduction is supported by the observation that the response vanishes when the EMT probe is removed from the nerve cord.

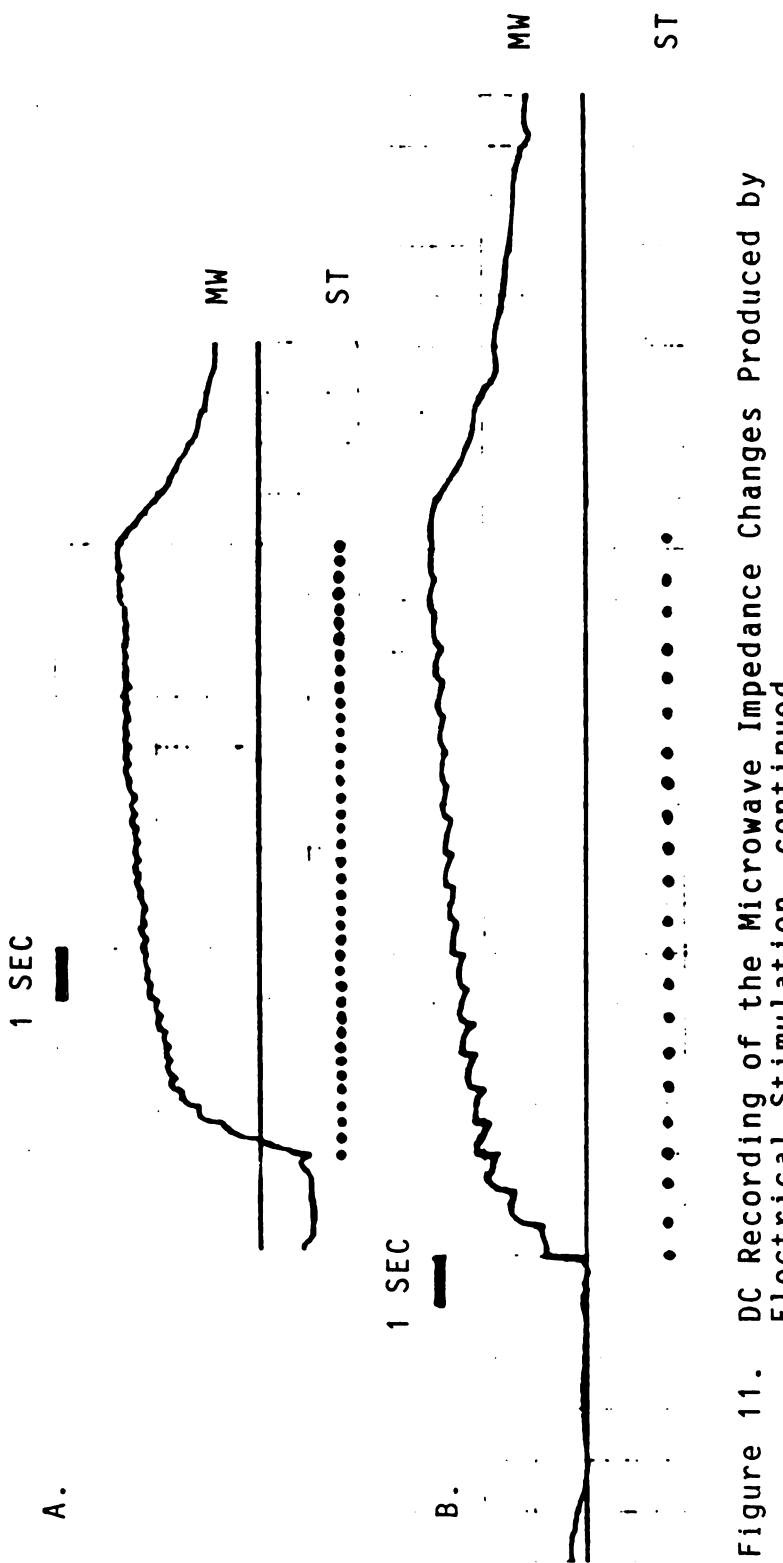
Figures 10 and 11 were obtained by the same means as Figure 9, except that the EMT was connected to a DC amplifier and a DC chart recorder. These figures illustrate more clearly the extended time course of the MW response of the stimulated nerve cord. In this case, the time course of the response to a stimulus is seen to be approximately exponential with a time constant in excess of two seconds. The rapidly varying parts of the response seen clearly in Figure 9 are lost by the recording method used in Figure 10. When pulse trains are delivered which have repetition rates in excess of once per two seconds, the responses overlap and exhibit summation. This is visible at B. of Figure 10 and at A. of Figure 11. The rate of summation increases with the stimulus pulse repetition rate.

Taken together, Figures 10 and 11 show that the microwave impedance changes of stimulated nerve cord are primarily slowly varying phenomena as compared with the unit DC Recording of the Microwave Impedance Changes Produced by Electrical Stimulation. Figure 10.

The cockroach nerve cord was examined with the EMT in the same manner as was used to record Figure 9, except that DC amplification and recording was used. Consequently, the DC level is observed to shift in response to the electrical stimuli (indicated by the dots). The DC level decrements in an approximately exponential manner following each response. The time constant for this decrement is in excess of two seconds and cannot be seen in Figure 9. In A., pulses are delivered once every three seconds, and some summation of the responses is observable. In B., the pulses are delivered about once per second so that the summation is more obvious. This record is continued in Figure 11 where pulses are delivered at a rate of three per second.



DC Recording of the Microwave Impedance Changes Produced by Electrical Stimulation. Figure 10.



DC Recording of the Microwave Impedance Changes Produced by Electrical Stimulation, continued.

action potential. The results shown in Figures 10 and 11 should be compared with the discussion of Figure 6, for the microwave responses of the electrically stimulated nerve cord are somewhat similar to the microwave responses of the electrically stimulated saline/mineral oil interface. In both cases, the MW signal is of much longer duration than the stimulus, and the responses can summate and decay exponentially. This similarity is discussed in more detail below.

Figures 9, 10, and 11 are distinct from the other recordings presented in this thesis: they are the only examples where electrical stimulation was used to elicit a response. The remaining figures show spontaneous activity, in one case elicited by non-electrical means. This restriction was applied to the experiments in order to ensure that the preparations were totally immobilized while the recordings were taken. When electrical stimulation was used. some visible changes could always be seen to occur, especially in the vicinity of the stimulating electrodes. Figures 9, 10, and 11 were obtained with great care so that muscular causes of these responses could be ruled out. Nevertheless, it was deemed important to exhibit MW responses from a system in which even the possibility of muscular activity was removed. Such a system is provided by the spontaneous activity of the cockroach nerve cord. In practice, the nerve cord is surgically stripped away from the surrounding muscular and respiratory tissue, as in

figure 8. All nerve fibers leaving the cord to innervate the body wall are cut. The thorax and head are removed, which also removes all legs, wings, and associated musculature. The cerci and the cercal ganglion are usually kept intact. Following this surgery, the nerve cord can be seen to be motionless under the dissecting microscope. In particularly robust preparations, the EL signal will be sustained for several hours, and MW signals can be detected for nearly this long. The spontaneous activity provided by such a preparation is certainly not the normal activity of the intact animal, but it is non-muscular.

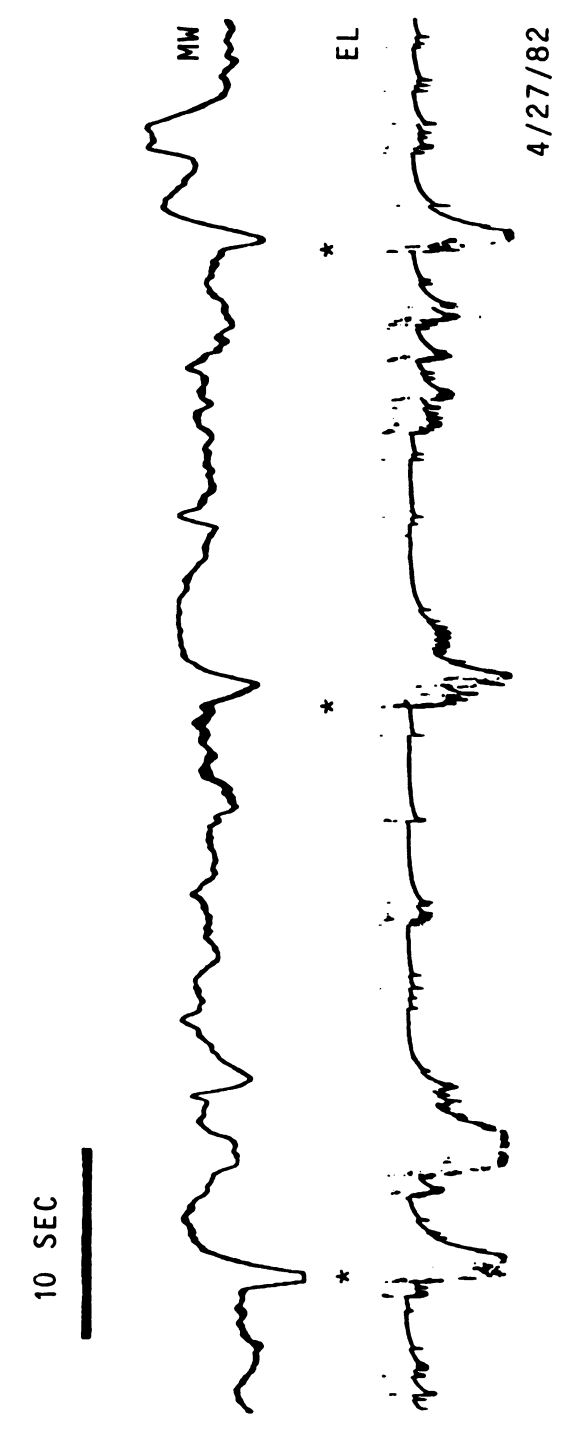
Figure 12 shows the simultaneously recorded EL and MW signals from the nerve cord prepared as just described. Figure 13 is an enlargement of a section of Figure 12. Together, these figures show that the EL channel is capable of detecting unit action potentials but that the MW channel is not. The spontaneous units are discernable in the EL signal, although they are somewhat indistinct. These spikes are readily detectable using an audio monitor or an oscilloscope. No evidence of unit spike activity can be found in the MW signal when displayed on an oscilloscope. As was shown above, this is not due to the limited frequency response of the EMT.

Although the unit action potentials do not show up in the MW signal, the density of spikes is exhibited somewhat in the MW signal. In the EL signal, the clustering of spikes yields a drop of the EL baseline. A similar baseline variation can be seen in certain parts of the MW signal. The regions marked with an asterisk (*) indicate moments during which an obvious similarity exists in the baseline variations of the two signals.

Because unit action potentials do not show up in the MW channel, it is convenient to filter the EL signal, since this has the effect of integrating over the spikes and smoothing the signal so that the MW and the filtered EL signals become more readily comparable. In practice, the EL signal is split into a raw electrical potential signal (REL) and a filtered electrical signal. This filtered signal is easily obtained by setting the frequency limiter switch of the IC-MP module to the low-pass mode (marked "mean"). This mean electrical signal (MEL) is then recorded.

Figure 14 shows that the comparison between the MW and the EL signals is indeed facilitated by filtering the EL signal. The raw EL (REL) signal is comprised of spikes which contribute to a baseline variation of unclear structure. The filtered EL signal (MEL) appears much smoother and is more easily compared with the MW signal. Both of the records shown in Figure 14 are from the same preparation under identical circumstances, and they were recorded only a few seconds apart.

Figure 15 shows the MW and the MEL signals from a single preparation where a few minutes has elapsed between the two recordings. Initially, the preparation is exhibiting



Spontaneous Activity of the Cockroach Nerve Cord as Detected by the EMT. Figure 12.

Spontaneous Activity of the Cockroach Nerve Cord as Detected by the EMT. Figure 12.

sound like a sharp snap in an audio monitor. Note that no evidence of individual spikes is visible in the MW signal. In the EL channel, the baseline drops when the spikes are clustered together, and a similar baseline variation can be seen in the MW signal at certain moments. These baseline variations in the EL channel are due to the charging of a capacitor in the chart recorder These have a duration of about one millisecond as seen on an oscilloscope and Action potentials are indistinct but visible as spikes in the EL channel. and do not appear on the oscilloscope screen.

*Indicates moments of obvious similarity of the signals in the two channels.

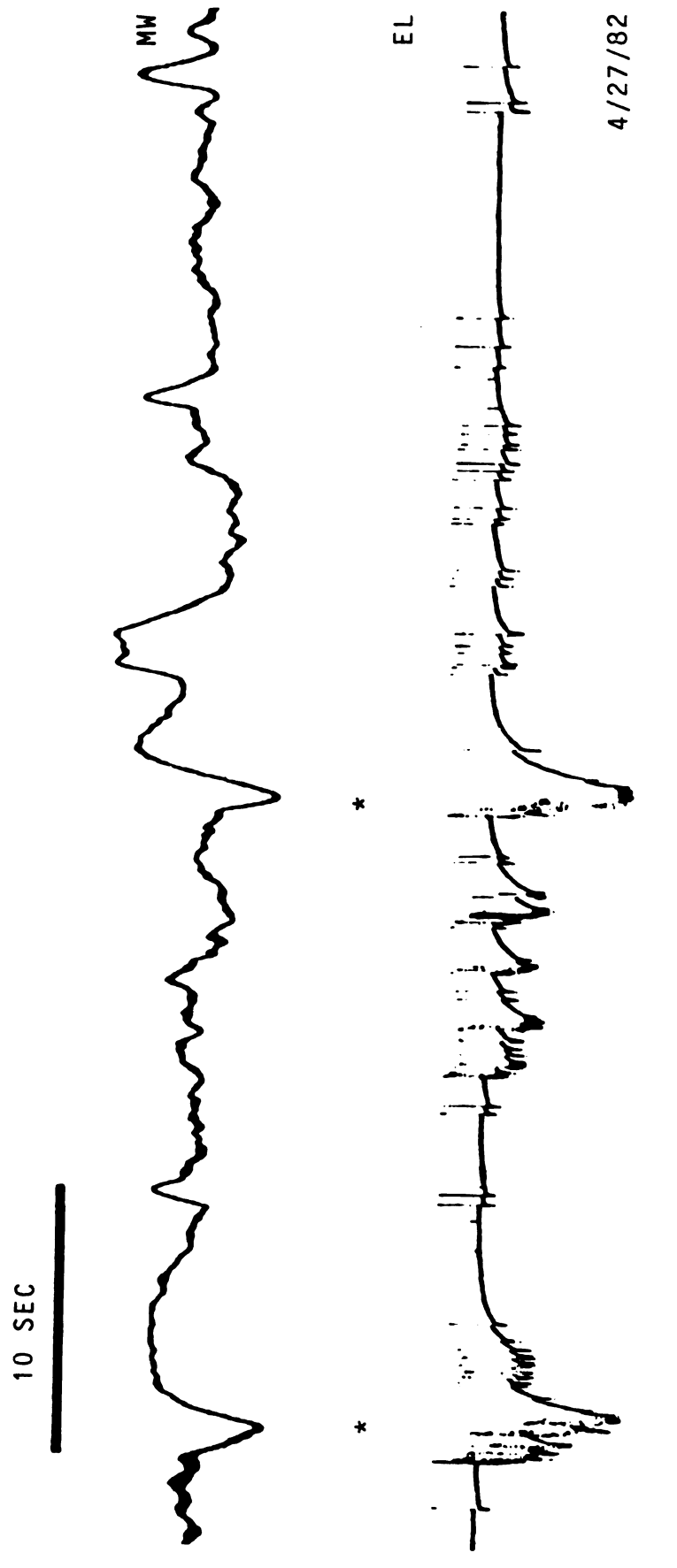
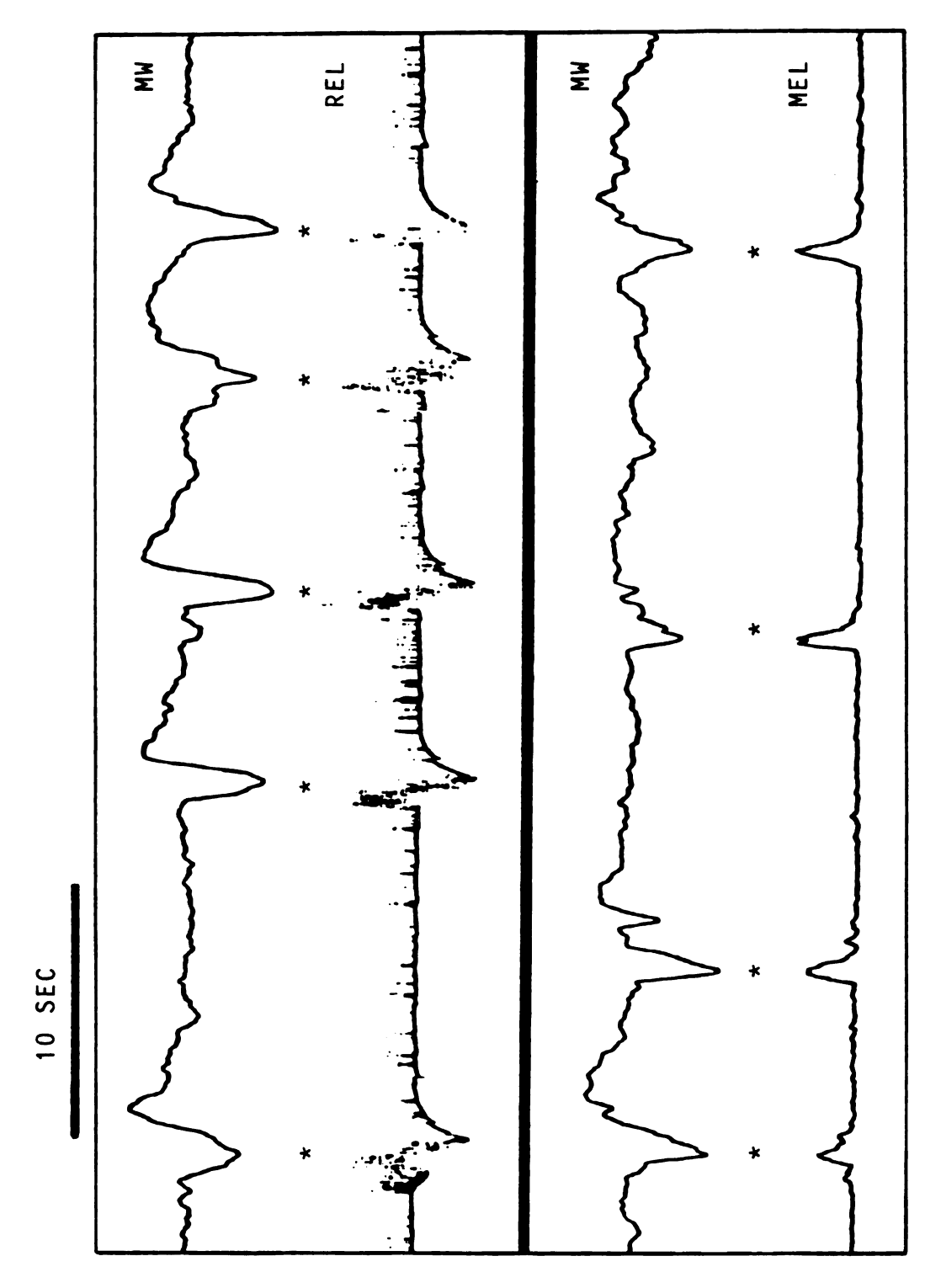
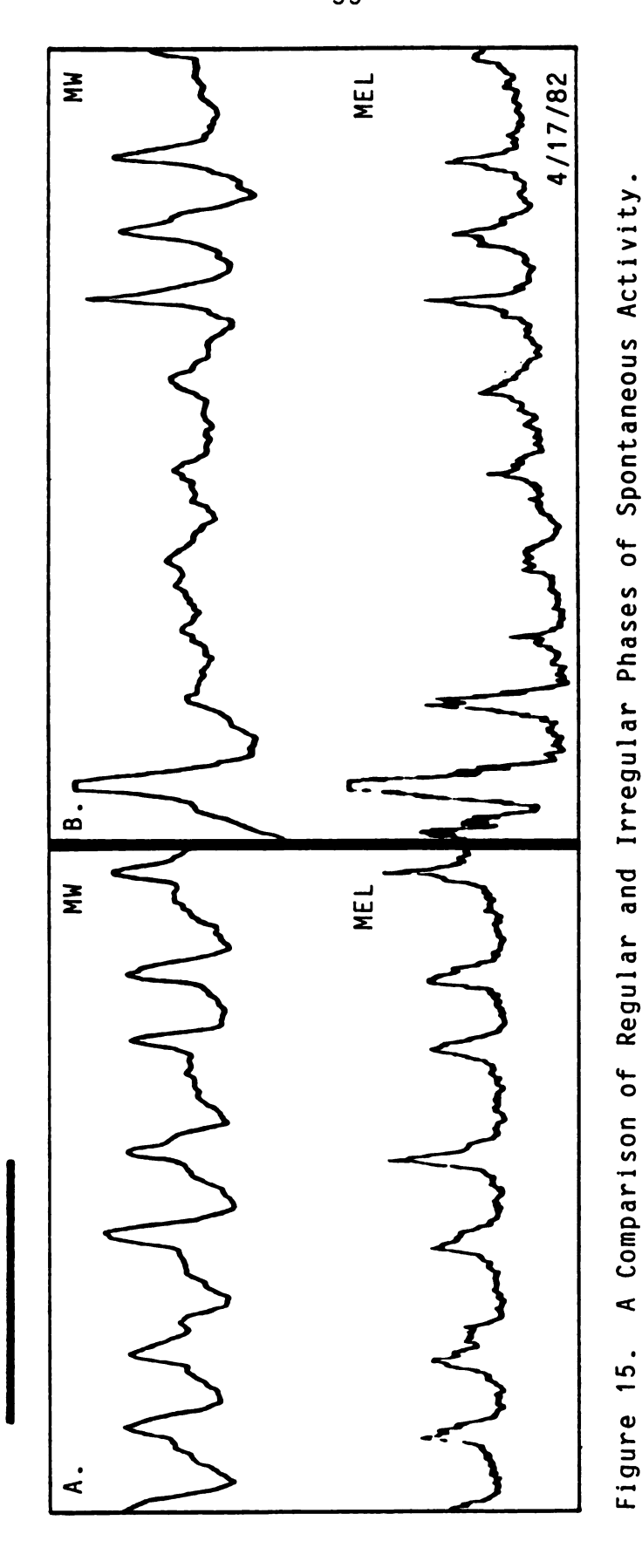


Figure 13. A 2× Magnification of Figure 12.

A Comparison of the Raw and Filtered EL Signals with the MW Signal. Figure 14. At the top are shown simultaneous recordings of the MW and the raw EL (REL) signals. At the bottom are shown simultaneous recordings of the MW and the filtered EL (MEL) signals. Both records are from the same preparation and were recorded under identical circumstances. Asterisks mark regions of obvious similarity in the waveforms of the two corresponding signals.



A Comparison of the Raw and Filtered EL Signals with the MW Signal. Figure 14.



10 SEC

A. shows a repetitive signal of fairly uniform amplitude and period. B. shows the signal from the same preparation after a lapse of a few minutes. Note the similarity in form of the MW and the MEL signals.

rhythmic activity of a regular sort; the period is on the order of two or three seconds. After a few minutes, the activity has become more variable so that the periodicity is compromised by relatively large variations of amplitude. Consequently, the EMT appears capable of monitoring functional changes occurring in the neural tissue. Again, an easily discernible similarity of the MW and the MEL waveforms can be seen, and the similarity can be seen not only in the regular periodicity but also in the variations of amplitude.

Figure 16 shows a longer segment of signals recorded from the same preparation studied in Figure 15, and Figure 17 shows a magnification of a section of Figure 16. Again, it can be seen that the MW and the MEL signals exhibit marked similarities of waveform. The two waveforms are not identical, however. The waveforms show similar variations in amplitude and rhythmicity, but the two signals differ in details. For example, Figure 17 shows a magnification of the prominent irregular feature in Figure 16. This feature (arrow) is grossly present in both signals, but inspection reveals that few, if any, of the excursions in the irregular region of the MW signal match those in the MEL signal. Certainly the two signals are not superimposable even though the resemblance is strong.

Figure 18 shows typical EMT signals from the cockroach nerve cord. The microwave impedance change (MW) is shown simultaneously with the raw electrical potential change

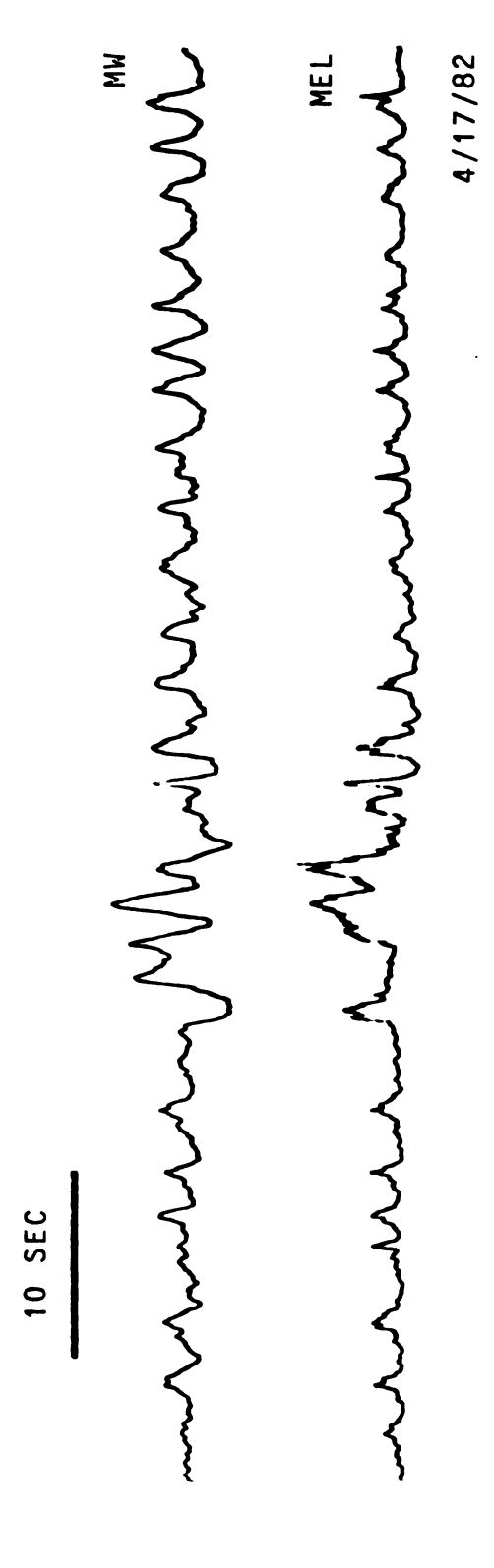


Figure 16. A Recording Exhibiting Good Correlation Between the MW and the MEL Signals.

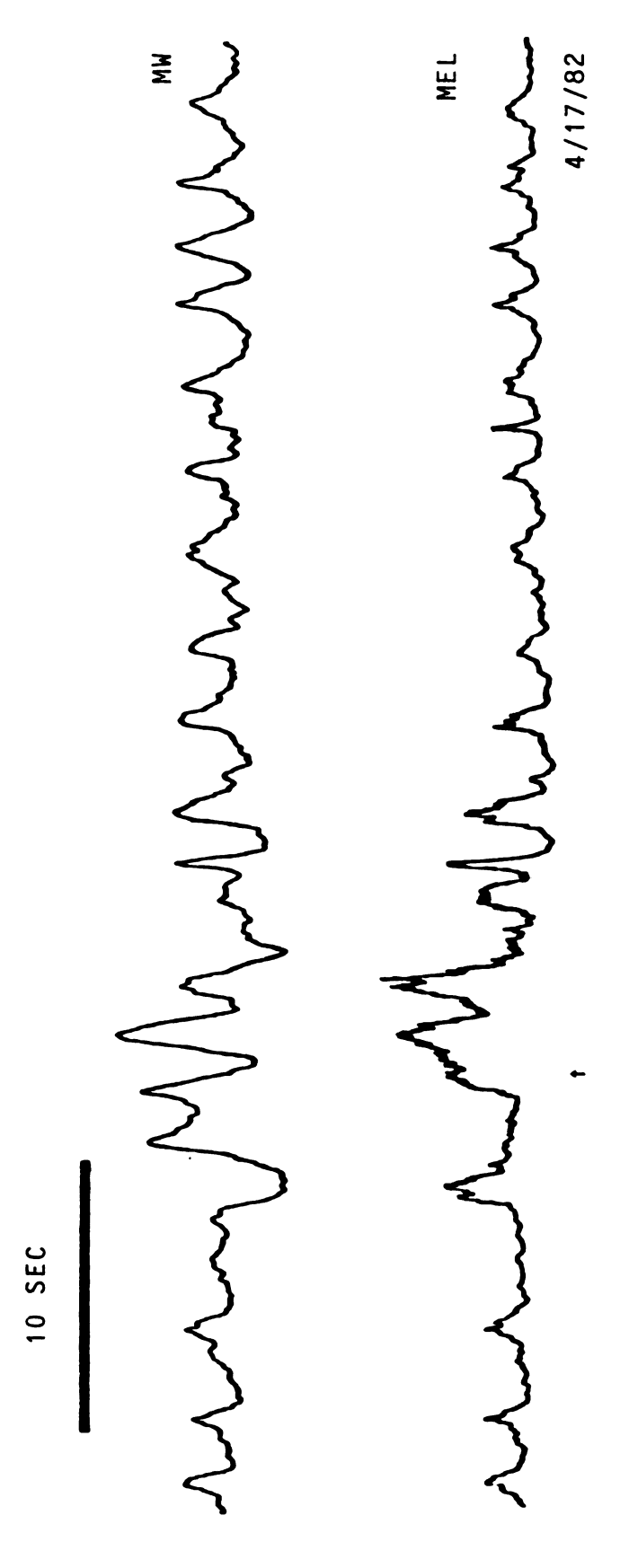
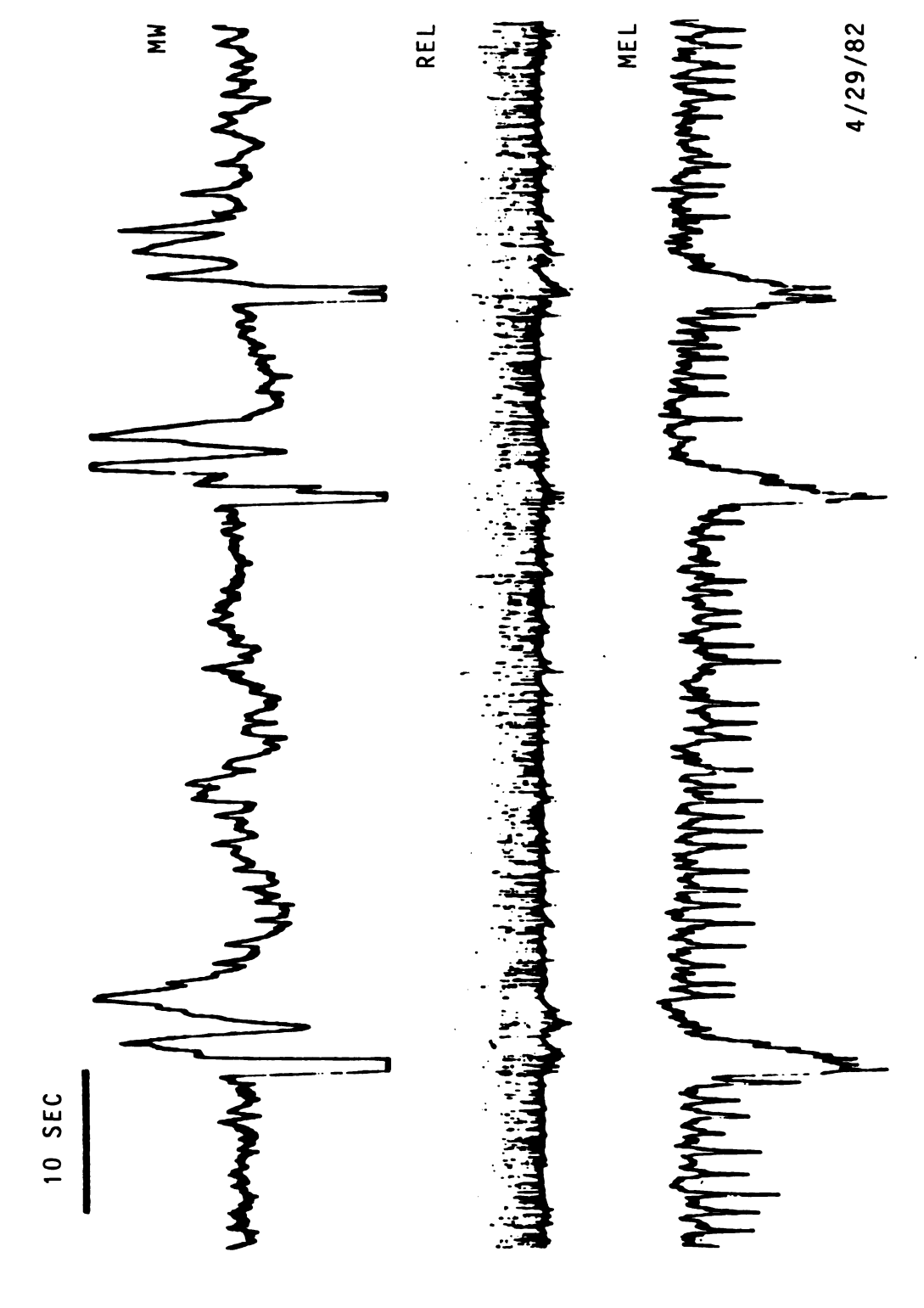


Figure 17. A 2× Enlargement of Figure 16.



A Comparison of MW, Raw EL, and Filtered EL Signals Figure 18.

(REL) and the filtered electrical potential charge (MEL). Note that the similarity between the MW signal and the MEL signal is much more obvious than the similarity between either of these and the REL signal. Again, the waveforms show similar features but are certainly not superimposable. The REL spike activity is almost homogeneous with faintly observable spike density variations in the region of the prominent MW excursions. This figure shows that it is not the presence of spikes but rather the changes in the spike density which appear to underly the microwave impedance changes.

Figures 19, 20, and 21 are intended to be studied as a group. These figures illustrate typical EMT signals from the nerve cord. These recordings were made under identical conditions, as much as possible, on three different days, each day using a fresh animal. These figures are presented to show the consistency of the type of signals provided by the EMT when cockroach nerve cord is investigated. Figure 19 shows again that it is the integrated spike activity, not the raw spike activity, which usually correlates best with the microwave impedance changes. Note that the greatest variations in the raw electrical spike signal have few or no correlates in either the MW or the MEL signals. it appears that a filter network with an appropriately long time constant is capable of converting electrical potential variations into signals which look strikingly similar to the microwave impedance changes. This point will be



Figure 19. Typical EMT Signals.

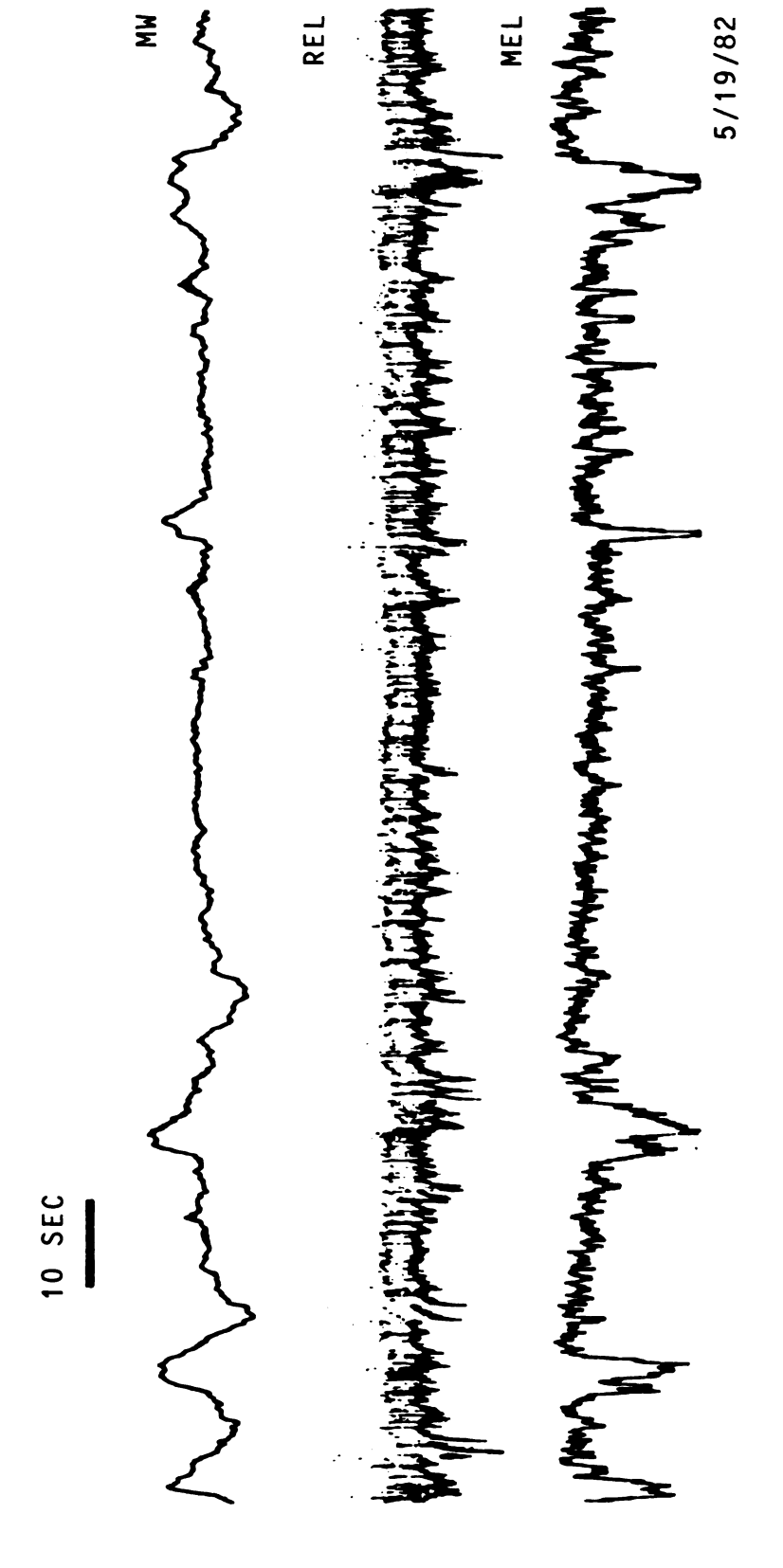


Figure 20. Typical EMT Signals.

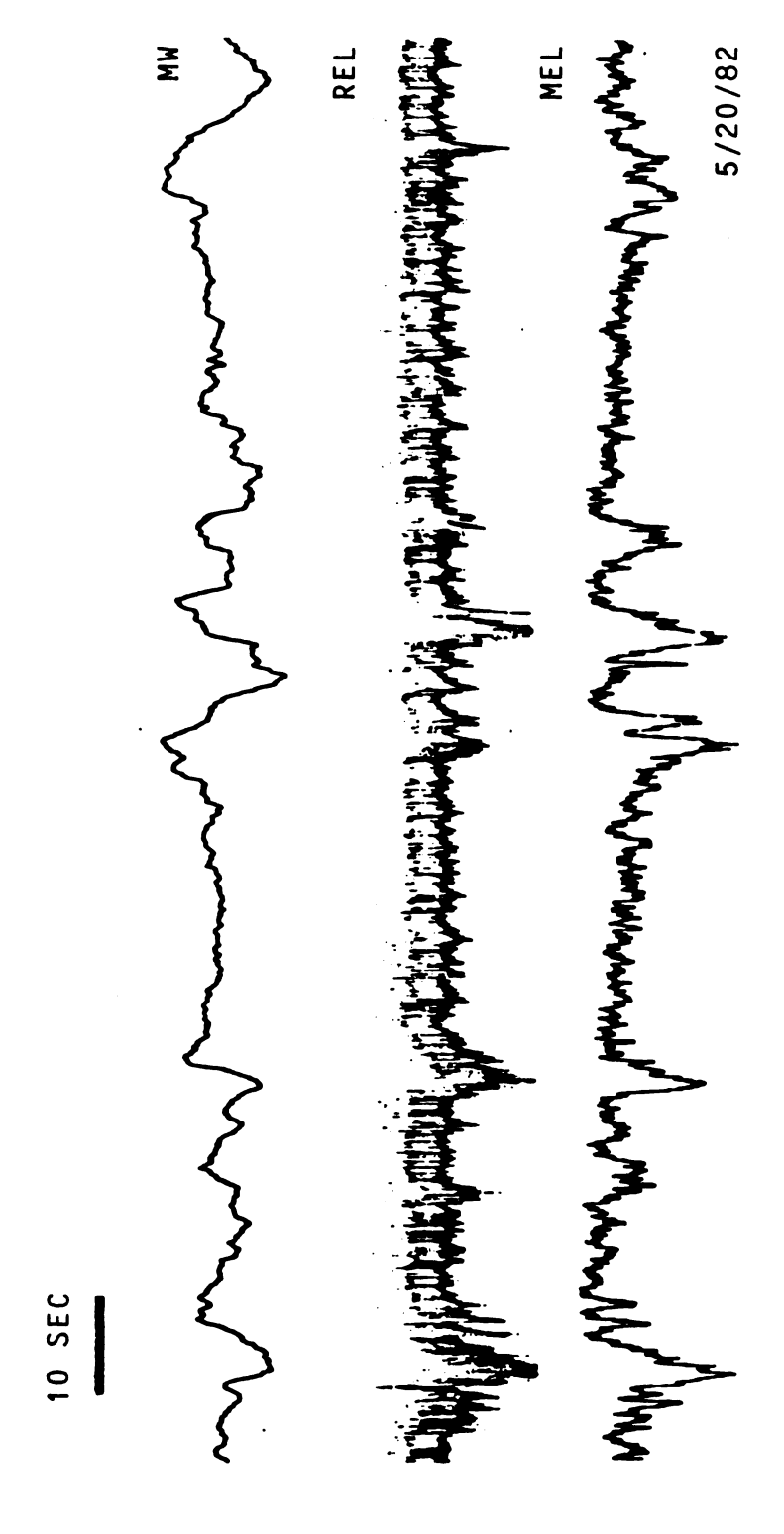


Figure 21. Typical EMT Signals.

reiterated below in a discussion of the mechanisms by which neural activity may appear as a variation of microwave impedance.

CHAPTER 3

DISCUSSION OF THE RESULTS

At this point, it is appropriate to review briefly the information presented above so as to permit a unified discussion of the significance of the experimental data. the Introduction, a short history of the impedance techniques used in neurophysiological investigations was presented, and it was indicated that frequencies higher and lower than microwave have been used with some degree of success to detect neural activity. As a consequence, a means was sketched by which an instrument could function so as to allow an investigator the possibility of detecting neural activity as a microwave impedance variation. Such an instrument has been constructed, and its basic operating principles were outlined in the Introduction. This instrument, the EMT, allows simultaneous monitoring of the microwave impedance changes and changes in the electrical potential of small samples. The EMT was applied to bulk-phase systems, to interfacial systems, to systems of ionized gas, and also to the nerve cord of the cockroach.

The stated purpose of the present study is to provide evidence to support the hypothesis that neural activity may alter the microwave impedance of the tissue, and such

evidence has been presented above. Thus, the primary issue at present is not whether microwave can be perturbed by neural activity in the general sense defined above but whether the microwave impedance changes which are observed can be explained or analyzed in terms of basic biophysical principles. The biophysical principles in question are illustrated in Figures 4 through 7. In Chapter 1, these figures were presented to show what kinds of systems do and do not yield microwave impedance changes. In the present section, the changes occurring in these physical systems are related to the changes observed in active neural tissue, at least in a general way.

The first topic needing further discussion is the basic mechanism by which the microwave impedance changes are detected by the EMT, i.e., resonance perturbation. Figure 4 shows the tiny motions of a needle yielding resonance perturbations. The mechanism by which these perturbations can arise is simply explained by basic electromagnetic theory [20]. The needle surface represents a metal/air boundary, and the microwave field is always constrained to obey the boundary conditions that both the electric and the magnetic vectors must have components parallel to the interface which are identical on each side of the boundary. As the needle moves, the position of the boundary changes, and the microwave probe field is simultaneously distorted in such a manner that the boundary conditions are always satisfied. This distortion of the field lines within the

microwave probe field alters the resonance of the standing wave tube, and a MW signal is detected. Thus, Figure 4 shows that a moving, vibrating, or bending interface can perturb microwave. If a smoothly cylindrical needle was rotated about its long axis, little or no microwave perturbation would appear, because even though the needle is moving as a rigid body, the metal/air interface is not displaced with respect to the probe field.

Naturally, if the needle was made of plastic instead of metal, the microwave perturbation would be greatly reduced in amplitude since the strength of the interface would be less: plastic is more similar to air than is metal with respect to its electromagnetic properties. can be stated more rigorously by saying that any bulk medium possesses a dielectric impedance which depends upon the magnitude of the response of the material to an impressed electromagnetic field of given frequency. When two bulk media are joined by an interface, the dielectric impedance is altered upon crossing the interface, and the magnitude of the alteration depends upon the difference between the bulk impedances. The strength of an interface as a perturbative agency depends directly upon the change in dielectric impedance seen in crossing the interface. If both media are identical, the interface has no strength and vanishes; if the bulk media are very different (as in Figure 6), then a well-defined interfacial region exists which may perturb the probe field.

Insight into this situation may be had by reconsidering the boundary conditions obeyed by an electromagnetic field at an interface. Equality of the field components tangential to the interface, as discussed above, causes the fields on each side of the interface to maintain a certain formal continuity. Conversely, there is a definite formal discontinuity in the field components normal to the interface, and this discontinuity means that electrical charges reside at the interface. Appendix B gives a simple mathematical exposition, based on Maxwell's equations of electromagnetic theory, which support the following statements. The discontinuity of the probe field on each side of the interface is due to the presence of static and moving electric charges located in the interfacial region. The charges at the interface form an electrical double layer [21], which can be diffuse and complicated in its detailed structure. Because charge separation occurs at the interface, there is an associated interfacial electric field, and this field acts to provide a force on the interfacial charges tending to pull them together. This force can be expressed per unit interfacial area, and is then equivalent to an interfacial tension. This tension is determined by the product of interfacial electric field and the density of surface charge, but since the electric field is related to the charge density, it is apparent that the interfacial tension is ultimately dependent only upon the distribution of charges across the interface. Consequently, the

interfacial impedance can be changed ultimately by one means alone, which is by the alteration of the interfacial charge distribution, i.e., by alteration of the structure of the double layer.

The above discussion shows why no MW response is obtained from the system illustrated in Figure 5: there is no double layer to be modified by the applied voltage. The responses obtained from the system illustrated in Figure 6 are apparently due to the alteration of the double layer across the saline/mineral oil interface in response to the applied voltage. But to change the charge distribution at the interface is to introduce subtle structural alterations in the interfacial region. Such structural alterations are responsible for a host of electromechanical effects [21] including electrocapillarity, electroosmosis, electrostriction, electroplating, electrophoresis, and other well-known electrokinetic effects.

It is precisely because structural alterations at interfaces can be studied as variations of interfacial impedance that neurophysiologists have attempted to utilize impedance techniques, for it is tacitly assumed in such studies that the molecular basis underlying neural activity may be elucidated by the analysis of the observed impedance changes [22]. This point may be reiterated as follows: whereas recordings of electrical potential changes are readily available from neural tissue, these provide no intrinsic information about the associated structural

changes in the tissue. Volume conducted fields (e.g., stimulus artifacts) can be detected potentiometrically in regions distant from their source. By contrast, impedance techniques yield signals only when active tissue lies within the boundaries of the probe field, and furthermore, it is only the interfacial regions (i.e., membranes) within this volume of tissue which will contribute to the impedance signal. Impedance techniques can reveal membrane structural variations which are associated with neural activity but not potentials or other effects of this activity which are propagated into the bulk tissue or the surrounding medium.

Naturally, the interfacial configuration of neural tissue is more complex by far than the relatively simple interface illustrated in Figure 6. The boundary of every nerve cell represents an interface of complex shape, and the cellular interior is far from homogeneous. Furthermore, the processes of adjacent cells can be bundled and intertwined closely together so that even the extracellular space is not filled with a simple bulk-phase. Yet cell membranes are only of the order of 100 Å in thickness so that the degree to which neural tissue can be considered to be either bulk-phase or interfacial is problematical. In general, it can be said of neural tissue that it is somewhat like a colloidal system, with an enormous complexity of relations between interfacial elements. This is substantiated by comparing the dielectric impedance of samples

of neural tissue, other biological tissues, and suspensions of biological molecules. Examining the impedance of these over a wide frequency range, it is seen that in the kilohertz range, the dielectric impedances of biological tissue are higher than those of any other type of material, and this is characteristic of the structure of cell complexes [11]. Intact tissues have a higher impedance than do tissue homogenates, and normal blood cells have a higher impedence than do lysed blood cells. Consequently, as the membrane structure is decreased in its integrity, the dielectric impedance also drops. As another example of this, myelin is observed to confer upon neural tissue an increased dielectric constant primarily because myelin is constructed from the orderly overlapping of glial cell membranes. Thus, it is seen that even though neural tissue can be considered as a bulk phase possessing a definite dielectric impedance in the steady state, this impedance is largely determined at radio frequencies by the interfacial constitution of the tissue.

This situation can be further clarified by analogy with the system illustrated in Figure 7. In this case, a neon bulb is stimulated with a signal generator, and the microwave impedance change is registered using the EMT. Before the stimulus amplitude is sufficient to induce breakdown of the gas, the neon possesses no electric charge density and appears as a bulk phase (ignoring the glass wall of the bulb), and there is no observable MW signal.

Immediately upon breakdown, a MW signal appears at the same frequency as the applied voltage. Thus, it can be said that the non-ionized neon forms a bulk-phase background which contains electric charges and that the microwave modulation is due to the motion of these charges. The density of these charges is about 10¹⁰ per cubic centimeter [18] so that within the probe field there will be considerably fewer than a picomole of charges. Even so, the neon plasma can provide very large percentages of modulation of impressed microwave fields. Indeed, microwave impedance techniques enjoy wide use in the field of plasma physics.

In the case of neural tissue, a bulk-phase impedance can be visualized which is due to the average effect of all non-interfacial constituents as well as those interfacial constituents which are not subject to modification during the time that the impedance change is being monitored. Within this static background of essentially bulk-phase material exists the complex matrix of active neural membrane which is characteristic of the particular sample of neural tissue. The activity of these membranes appears to an impressed electromagnetic probe field as a complex structure formed of spatially and temporally variable electrical double layers. The double layers have a thickness of about 100 Å. At rest, the potential establishing the double layer may be on the order of 100 mV. Consequently, the trans-membrane electric field in the resting state may approximate 10^7 volts per meter. This corresponds to a

charge density of about one picomole of charges distributed over one square centimeter of membrane [2]. When membranes are stacked, bundled, and folded together in the structure of the neural tissue, the surface area within a volume rises rapidly, as also does the charge density contributed by the double layers. For example, a section of nerve measuring 1 cm in length and containing 1000 fibers each measuring 10 microns in diameter contributes in excess of 3 cm² of membrane. Thus, neural tissue may be considered to possess an adequate number of electric charges per volume so as to modulate an impressed microwave field, provided that it is fair to compare neon plasma with neural tissue.

In fact, however, the charge distribution in a plasma bears no formal similarity to the electrical structure of neural tissue. Plasma is the simplest electrical medium conceivable, for it is nothing else than a collection of charged particles. On the other hand, neural tissue easily ranks as one of the most complex media known, primarily because of the extensive elaboration of neural processes. The basic electrical structure of neural tissue is the plasma membrane of neurons, and it is precisely the complex organization of this membrane which is so distinctive of neural tissue. It is therefore evident that even though neural tissue may easily contain as great a charge density as a neon bulb, it is not necessarily true that neural tissue may be as efficacious as a neon plasma in producing modulations of a microwave field. This is because the

charges in a plasma are primarily free electrons whereas the charges in neural tissue are bound in various ways to the neuronal membranes, and the chemical species constituting the interfacial charges are of uncertain composition. Thus, it is both an appropriate density of electrical charge and an appropriate mobility of the charges which will determine the competence of neural tissue for providing modulations of an impressed microwave field. As a result of the above considerations, it is evident that the question of whether or not neural tissue can modulate an impressed microwave field cannot be settled by arguments based on the responses of the physical systems illustrated in Figures 4 through 7. This question must be settled by resort to experiment, and the results of the appropriate experiments have been given above. A microwave probe field is indeed modulated by the activity of the cockroach nerve cord, and at this point, it is appropriate to assess the mechanisms by which this is possible. As indicated above, two possible mechanisms exist:

- (a) The tissue is mechanically distorted by some muscular agency so that in effect the microwave modulation is similar in kind to that depicted in Figure 4.
- (b) The microwave modulation is effected by an electrically induced alteration of the interfacial regions (i.e., membranes) within the tissue, as illustrated in Figure 6.

It was stated in the Discussion of the Experiments that the neural tissue investigated in this study was surgically prepared in such a manner as to eliminate muscular activity. To the degree that this is incorrect, the results of this study may be in error. Assuming for the moment that all muscular activity has indeed been removed, the mechanism becomes apparent whereby a microwave field can be modulated by neural activity, and this is electromechanical structural alteration of the interfacial regions as described at length above.

The discussion turns now to a difficult question, i.e., the verification that all muscular activity has been removed from the preparation. An obvious method is the use of a dissecting microscope to view the preparation while recording the signals. An alternative method is to pass a small light beam over the nerve cord to register any displacements of the tissue as a change in the output voltage of a photodetector diode. In this study, both of these methods were employed. It was rapidly determined, however, that the transverse light beam technique suffered from a number of faults, in particular that the sensitivity of this technique as compared to the EMT technique was not known as regards the detection of muscular activity. It was found to be fairly easy to arrange things such that no deflection of the light beam was seen when a definite MW signal was detected. This is somewhat inconsequential, however, since the light beam may not have been arranged

optimally with respect to the tissue. And after all, visual inspection offers a superior detection of optical deflections when compared with the response of a commercial photodiode.

Consequently, the data presented above was inspected visually using a dissecting microscope during recording. These data were selected from a considerably larger number of recordings obtained over a period of some months. preparations from which these signals were recorded were inspected for visually detectable motions corresponding with the recorded MW signal. In general, it appears to be very easy to obtain MW signals from the nerve cord of the cockroach if any muscular activity is present; however, this type of signal does not necessarily yield similarities in the waveforms of the MW and EL channels. This is a completely reasonable result, since muscular motions will generally arise from activity of the somatic musculature at a point distant from the recording site along the nerve. The neural activity initiating the muscular activity may be originating at a distant locus and for that reason be poorly represented in the EL signal. Therefore, gross motions (i.e., due to muscular activity) of the nerve cord cannot be expected to produce similar signals in the MW and the EL channels in general, and this is verified experimentally.

Although the gross motions of the nerve cord could always be removed by surgery, it was frequently noted that

microscopic motions in the region of the surface of the nerve cord could still be observed. Usually these dynamic characteristics of the tissue were detectable only as faint modulations of reflected light or subtle distortions of the surface of the cord. These phenomena could be compared with the microwave signal by marking on the chart record the occasions during which microscopic motions could be seen, and it was often found that the more prominent MW excursions occurred during the observation of some microscopic activity in the vicinity of the EMT probe tip. As this seemed to represent a source of error in the data. great pains were taken to prepare nerve tissue which was absolutely free of visible modulation as seen under the microscope yet which was sufficiently functional as to yield signals in the MW and EL channels. Figures 22 through 24 show the results which were obtained during such time as it could be stated unequivocally that no visible activity occurred in the vicinity of the EMT probe tip. These can be compared readily with the preceding figures since the overall result is quite similar. Again, MW signals can be obtained spontaneously or by stimulation of the cerci (Figure 23), and again, these bear a striking similarity to the filtered EL (MEL) signals.

Consequently, it seems fair to state that MW signals are indeed detectable even when the nerve cord is subjected to severe surgical manipulations to remove all visible signs of activity. Of course, the surgery has deleterious

EMT Signals Obtained with No Visible Activity of the Tissue. Figure 22.

This record was taken under identical conditions as were the other recordings presented above, except that it was certain that no motions of any kind were visible under the dissecting microscope. Such data is more difficult to obtain than that in which restriction is made only to muscular motion.

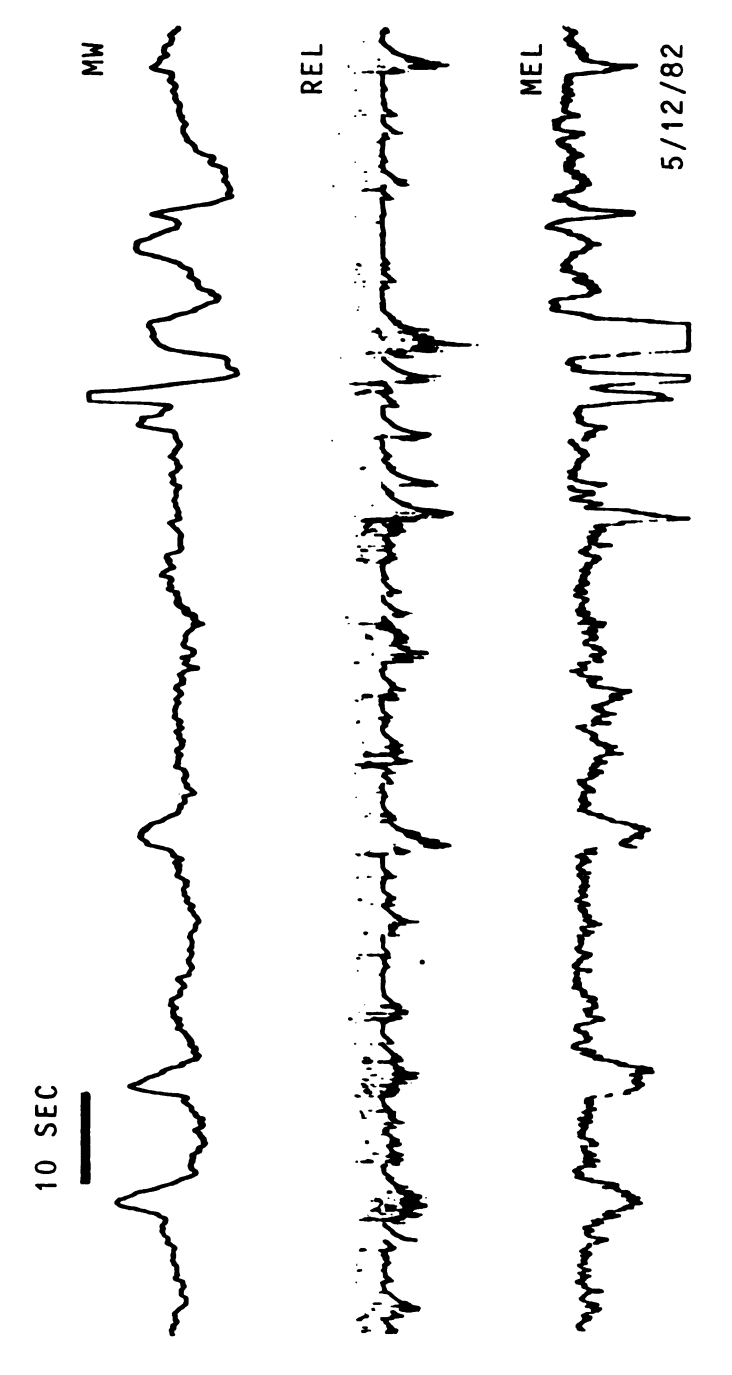
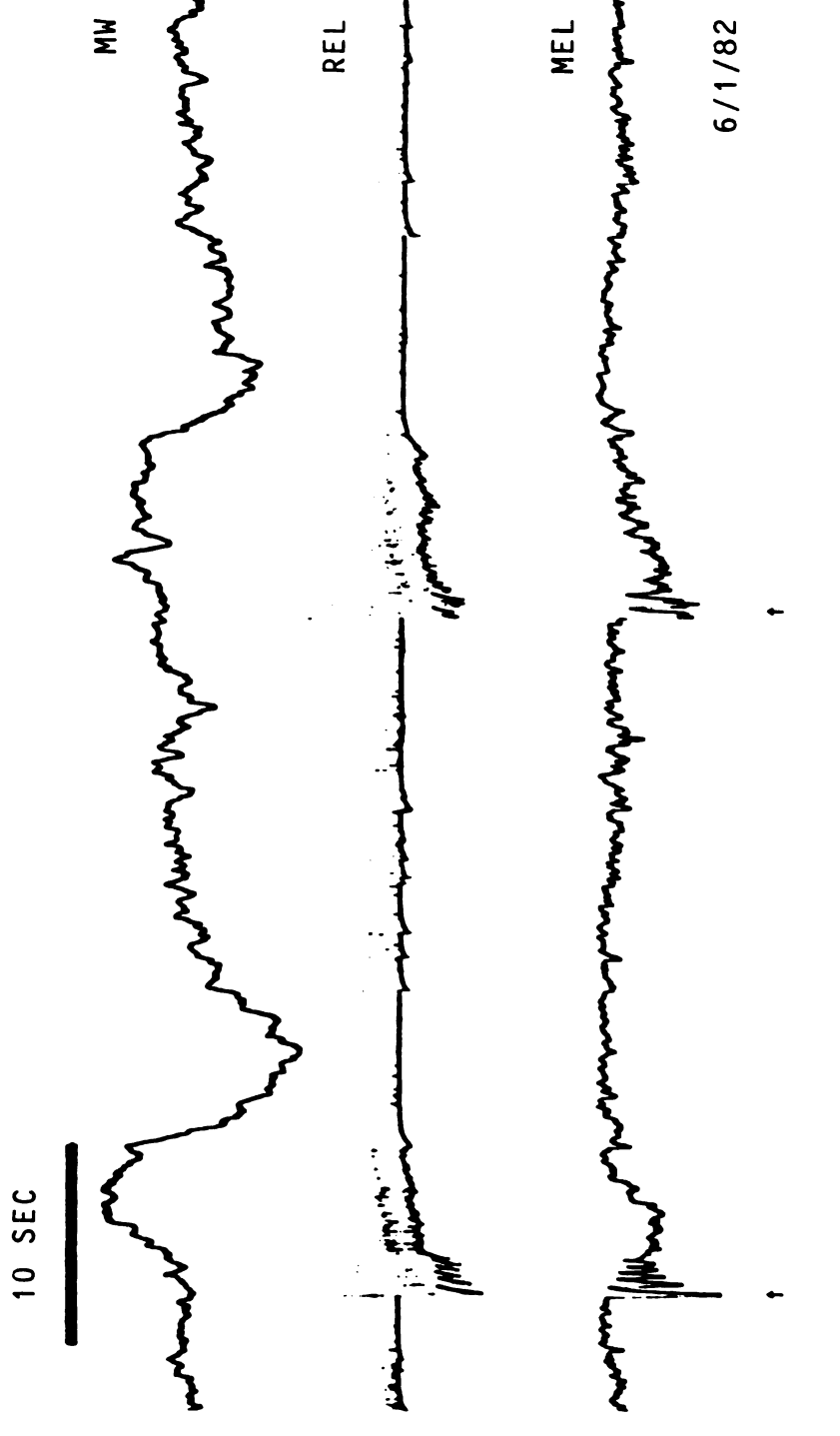


Figure 22. EMT Signals Obtained with No Visible Activity of the Tissue.

Responses to Stimulation of the Cerci with No Visible Motion of the Nerve Cord. Figure 23.

Puffs of air were delivered onto the cerci by means of a pipette. The onset of the stimuli are indicated by the arrows. The nerve cord was inspected under the dissecting microscope during recording so that it is certain that no visible motion of any kind occurred. The MW signal appears to follow the cessation of the EL signal.



Responses to Stimulation of the Cerci with No Visible Motion of the Nerve Cord. Figure 23.

Typical EMT Signals with No Visible Motion of the Nerve Cord. Figure 24.

This figure was recorded while the tissue was visually inspected under the dissecting microscope to verify the lack of visible activity. Notice that the major peaks are not superimposable in the two channels, yet there is a definite relationship between the signals. This is typical of the results obtained with the EMT. Although the EL and the MW signals reveal common features, it certainly cannot be claimed that the two channels provide identical information about the activity of the neural tissue.

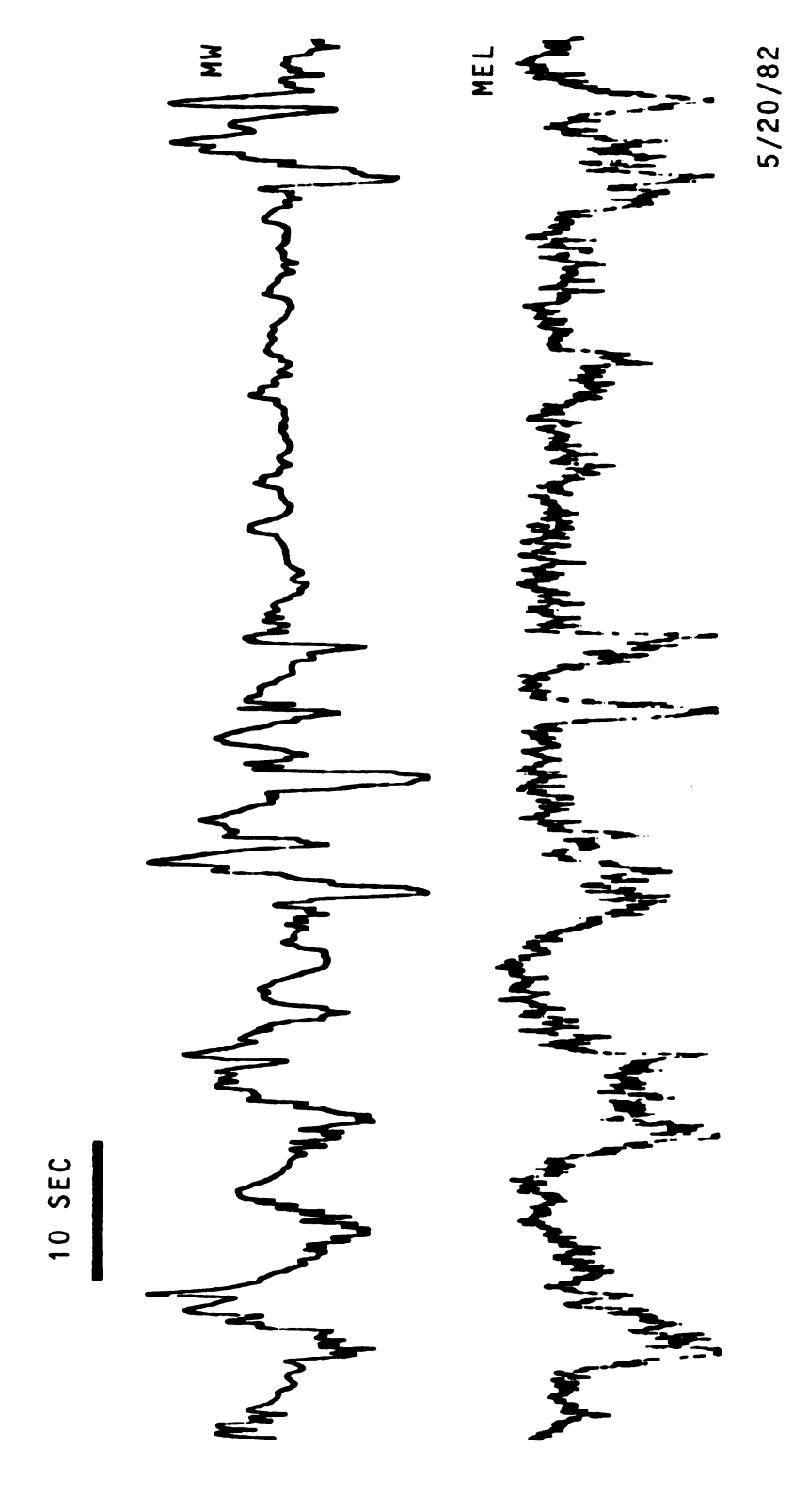


Figure 24. Typical EMT Signals with No Visible Motion of the Nerve Cord.

effects on the tissue so that, for example, Figures 22 and 23 were obtained only after great persistence. In other words, the same manipulations which yield no visible activity in the nerve cord also decrease the ability of the nerve cord to modulate a microwave field. Even so, by examining a sufficiently large number of preparations i.e., a few dozen), it has been possible to record MW signals in the absence of visible changes. This means that even if muscular contamination exists in some of the data shown in this thesis, examples can be given where this would definitely appear not to be the case, and these examples are similar in appearance to the rest of the examples shown above.

The most difficult experimental problem faced in the work described above was that of obtaining recordings which clearly illustrate positive correlation between the MW and EL signals. The present thesis shows many examples of such correlations, but these were chosen from a batch of recordings, at least an order of magnitude more numerous, which illustrated the correlations much less convincingly. More numerous by another order of magnitude were the recordings which showed no observable correlations at all, even though these exhibited activity in the MW and the EL channels. One simple reason why such signals fail to correlate is that the EL signal may contain contributions from action potentials which are occurring on neuronal processes which lie outside of the probe field.

The correlation between the MW and the EL signals was enhanced substantially by one device only, i.e., the use of a filter to convert the EL signal into a smoother, more slowly varying waveform (MEL). The use of this filter, which is a feature of the chart recorder used in this study, was of much greater importance in obtaining convincing records than was any particular surgical method, choice of physiological saline solution, selection of particular animals, or any other factor. It is of some importance, then, to understand the significance of this filtering technique. The raw EL (REL) signal exhibits features having frequencies in the kilohertz range (i.e., spikes). MW signal exhibits frequencies between 0.1 Hz and about 10 Hz. Consequently, direct comparison of these gives generally unconvincing results, i.e., a non-partisan observer would often fail to notice any particular similarities between the signals. By contrast, as shown above, the MEL and MW signals can be strongly similar in appearance. Formally, this is due to the fact that the filtered electrical signal has frequency characteristics similar to the microwave impedance signal.

More significant, however, is the fact that the filter indicates a mechanism by which the electrical activity of the tissue yields a microwave impedance change. The operation of a low-pass filter depends upon the existence of a large capacitance to provide an electrical inertia, i.e., the response time of the circuit is slowed. When spikes

are passed through such a filter, the spikes are integrated to yield a signal proportional to the spike density, and the MEL signal thus represents variations of the spike density. But this tendency of the tissue to integrate electrical activity in the generation of a microwave impedance change has been demonstrated several times above, in particular in Figures 9, 10, 11, and 18. Furthermore, this same kind of slowly varying MW response is exhibited by the system illustrated in Figure 6. The principal feature of the MW signal, when compared with the raw electrical recording, is its apparent inertia.

The origin of this inertia can be traced to the fact that the interfacial regions, i.e., those regions responsible for yielding impedance changes as a result of electrical activity, consist largely of bound charges (polarization charges). In the motion of bound charges, there is an implied structural change in the interfacial region, and this structural change must occur more slowly than a rearrangement of free charges (e.g., as in a neon plasma). A structural change in an interfacial region is an electromechanical effect, and thus it is to be anticipated that any electrically produced impedance variation has mechanical components which restrict its frequency response. is important when it is recalled that often the MW signal could be observed to occur during the time when faintly visible microscopic motions were present in the surface of the nerve cord, even though all muscular components to this motion were removed. Consequently, it must be reiterated that the microwave impedance changes documented in this thesis, although apparently not due to muscular activity, may well be due to mechanical deformations or strains which result from alterations of interfacial structures in the neural tissue. Thus, the EMT may ultimately prove to be a tool capable of exhibiting on chart paper effects which could conceivably be detected by sufficiently acute visual inspection, although because these effects are so slowly varying and subtle, they might well be difficult to study without the use of the EMT.

CHAPTER 4 SUMMARY AND CONCLUSIONS

The purpose of the present thesis was to determine whether neural activity can appear as an impedance variation at microwave frequencies. This is of some interest because structural information about active neural tissue has been gained by investigators using kilohertz, infrared, and visible radiation. In the present study, a resonance perturbation technique was employed, and a single section of coaxial cable was used as a probe of electrical activity and microwave impedance. The results of the present study show that impedance variations are observed in the ventral nerve cord of the cockroach, and these signals bear a striking resemblance to the electrical activity especially when the electrical activity is filtered. Thus, the microwave impedance changes are more slowly varying than are the associated electrical signals. It appears that changes in spike density are required for detectable microwave impedence variations, i.e., clusters of spikes are detectable but the spikes themselves are not. This leads to the conclusion that spike density variations may have dynamic consequences which are qualitatively different than the effects of single spikes.

Visible changes in the neural tissue have been by far the greatest source of disconcert as this study was carried out, and the employment of impedance techniques at any frequency will always be hampered by the existence of these microscopic phenomena. As long as it is certian that these are not due to muscular activity, such changes are not necessarily a problem, for it is certain that the impedance of the tissue can be altered by electrical activity only in so far as structural changes occur in the electrical double layer configuration within the tissue, and these structural changes may well have visible effects. To the degree that such visible changes are electromechanical (but nonmuscular) in origin, new information about neural activity is indeed available using impedance techniques. For in this case, an instrument similar to the EMT could be used to record these faintly visible phenomena on chart paper simultaneously with the electrical activity. To the degree that such visible changes are of muscular origin, the impedence techniques are of considerably less utility, except, of course, in studies of muscular activity.

That electromechanical effects at interfaces can easily yield large microwave impedance changes while exhibiting only faint and indistinct visible changes was shown in the case of the saline/mineral oil interface. In this case, the interfacial inertia limits the frequency to less than 10 Hz. This same type of response can be obtained from a variety of electrified interfaces (in particular,

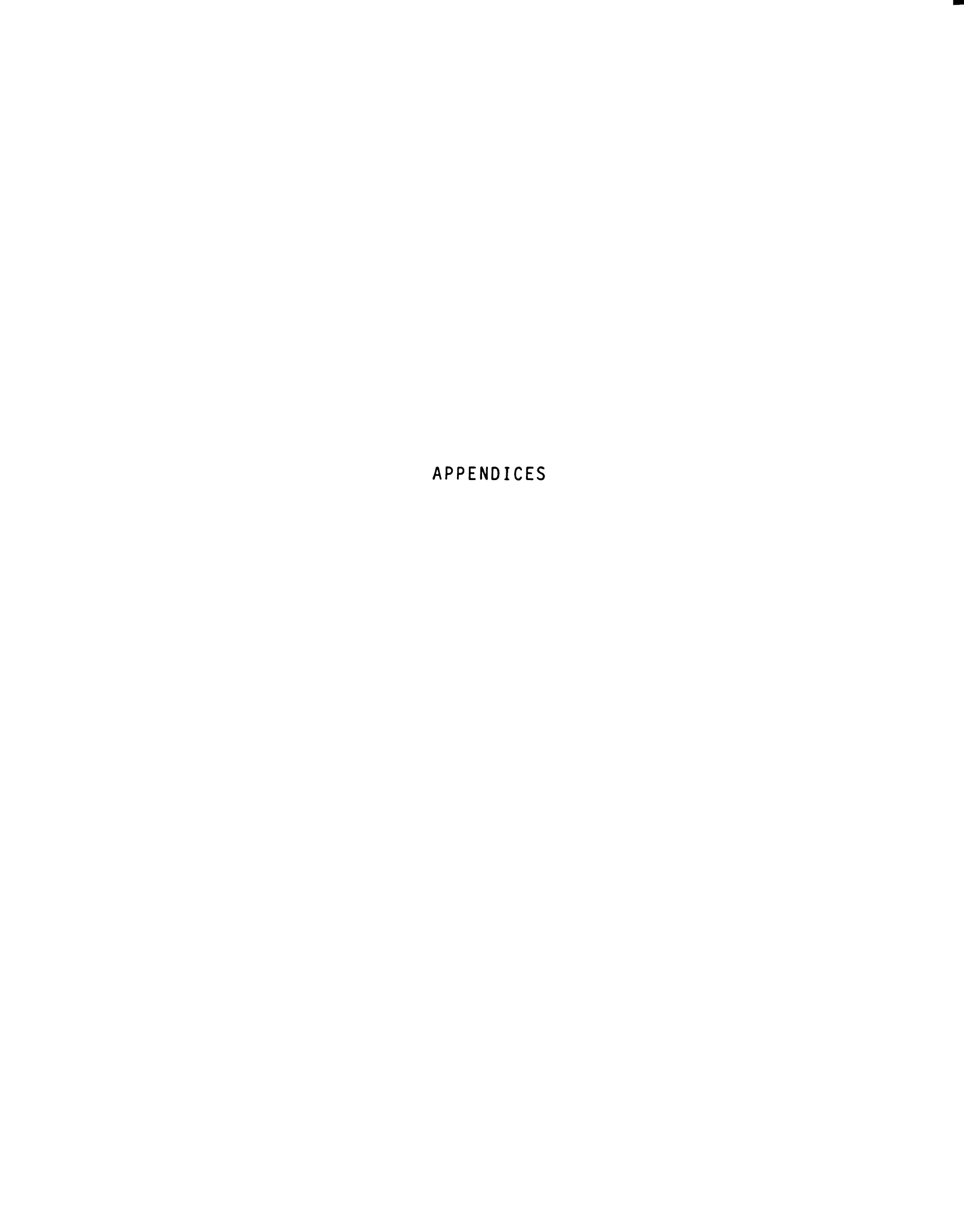
the saline/mercury interface which figures so prominently in the electrochemical literature). And this same type of response is characteristic of the neural signals presented in this thesis. Responses of the neural tissue as viewed in the microwave impedance signal invariably appear slow compared to the simultaneous unfiltered electrical activity. Filtering the electrical signal yields a wave form which often bears striking similarity to the associated microwave signal, even if this is not evident by inspection of the raw electrical record.

The relatively slow response of the impedance signal is due to an inertial property. Such an inertia can be introduced into an electrical circuit using a large capacitance, and this is exactly what is required to introduce visually obvious similarities in the electrical signal when compared with the microwave signal. But all interfaces are composed of electrical double layers and in this sense are like capacitors. Interfacial capacitance differs from the capacitance of ordinary capacitors as used in electrical circuits primarily in that the width between the double layers is not fixed. When this distance can be altered, an electromechanical effect is introduced, and this will have a natural response time which is limited by the inertia of the charges comprising the double layers. Interfacial capacitance is thus a non-linear and highly complex phenomena, since the capacitance is not constant when the applied field strength is varied. Increased field strength alters

the interfacial structure, and this introduces a relaxation process limited in its characteristic frequency by the inertia of the charged species.

At this point, it is appropriate to express the differences in the viewpoints of the physical nature of neural activity, as suggested by potentiometric studies versus impedance studies. Potential variations of neural activity are characterized by spikes (action potentials) which are recorded without fear of contamination by slight mechanical displacements. Consequently, the spikes and spike densities are conventionally viewed as counting events without dynamic consequence. This is also true of field potentials. Neurophysiologists often speak of information encoded in these signals as if these signals had no other effect than the expression of digital information. On the other hand, these signals produce no impedance variations, at least not at microwave frequencies. In order for the impedance of the tissue to be altered, neural activity must be envisioned to possess the possibility of dynamic consequences. Unless structural alterations of charged layers occur, no impedance variation is detectable. Whether these variations are visible or not is of secondary importance; these variations must be present in order to obtain an impedance signal, and presumably, any impedance signal observed at any frequency is still electromechanical in nature, even if it is difficult to see the deformations visually. One

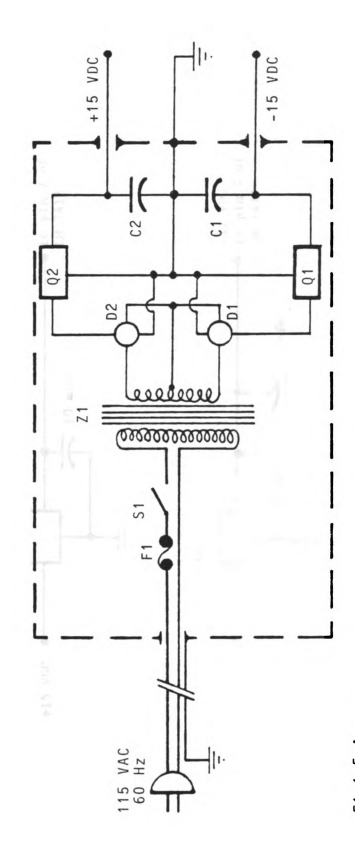
cannot have structural alterations in a condensed medium without mechanical strains.



APPENDIX A

SCHEMATIC DIAGRAMS FOR THE EMT

Figures A-1 through A-5 provide complete specifications for the construction of an EMT. This same design was used in the construction of the EMT used in this study. The particular features of this design include: stability and low noise in the power supply output; separate regulation of the voltage feeding the two amplifiers; a separate regulation of the voltage feeding the Gunn diode; AC coupled physiological amplifier with a gain of one thousand and a frequency response extending from 0.1 Hz to at least 5 KHz; and AC coupled amplifier for the standing wave tube in the EMT with a gain of 30 and a frequency response extending from 0.1 Hz to at least 5 KHz.



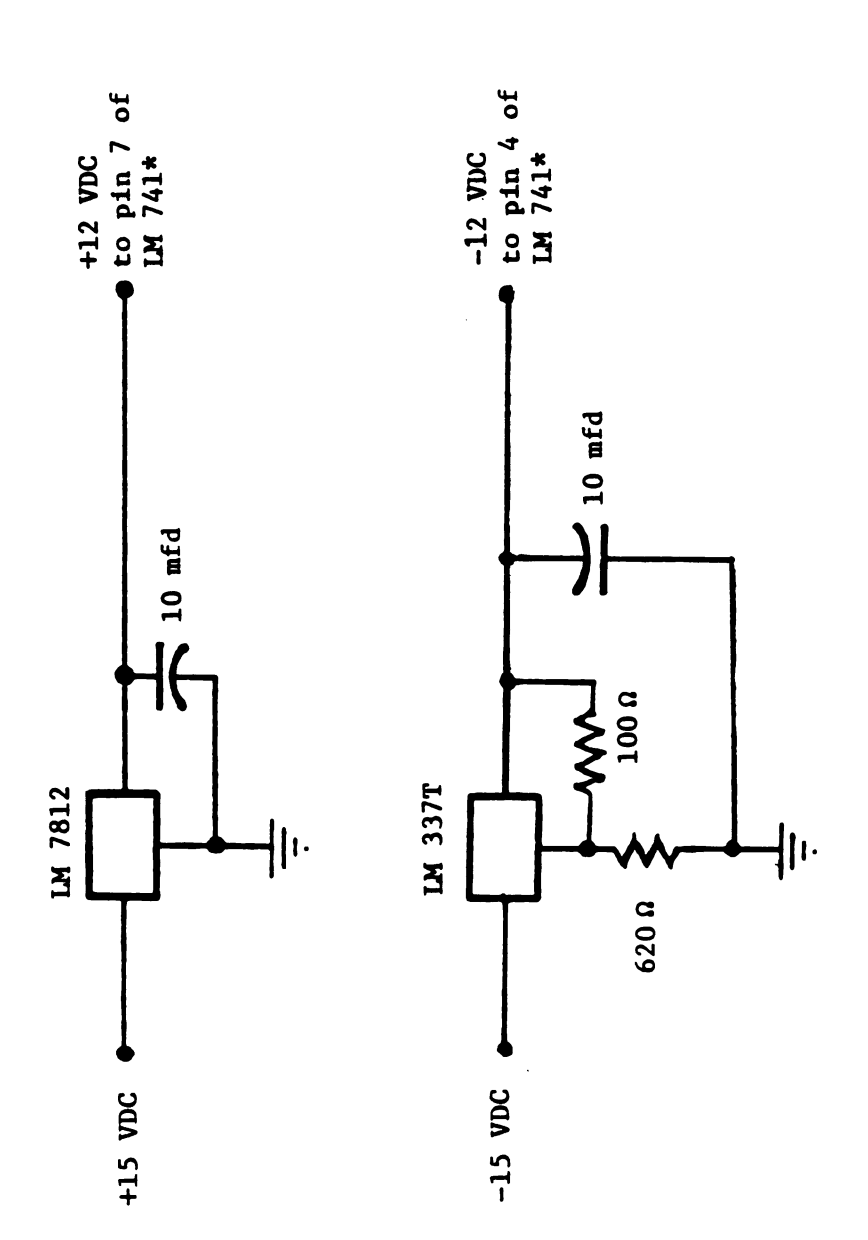
D2-Bridge Rectifiers Q1-LM 7915C Negative Voltage Regulator Q2-MC 78M15CT Positive Voltage Regulator C2-2200 mfd 50 Wy electrolytic

oggle 120 VAC 60 Hz; Sec.: 25 VAC 2 A center-tapped

S1-SPST 1 Z1-Pri.:

. 13

Schematic Diagram of EMT Power Supply. Figure A-1.



*Note: All LM 741's are connected in parallel.

Figure A-2. Connections from Power Supply to the Amplifiers.

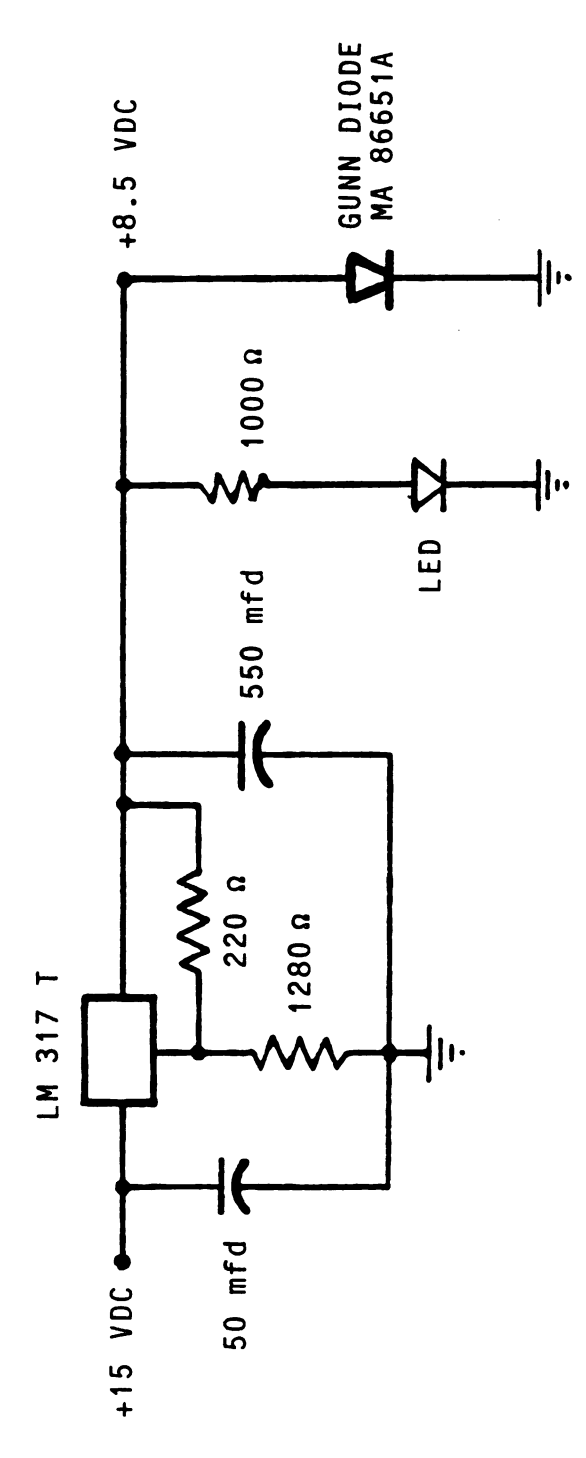


Figure A-3. Connections from Power Supply to the Gunn Diode.

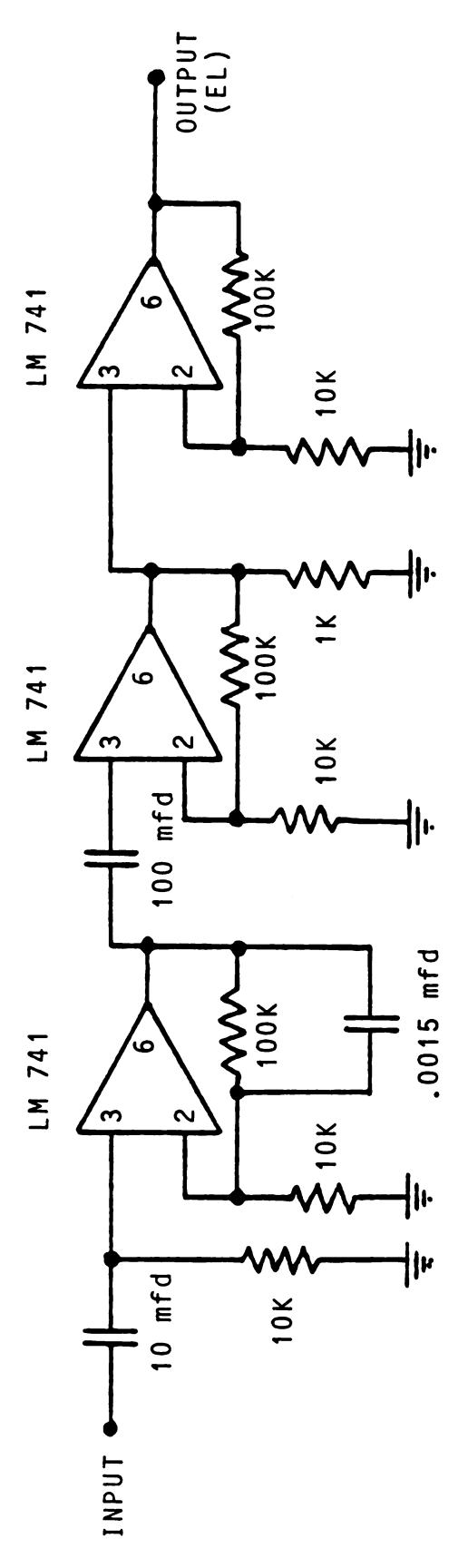


Figure A-4. Schematic Diagram of the EMT Physiological Amplifier Circuit.

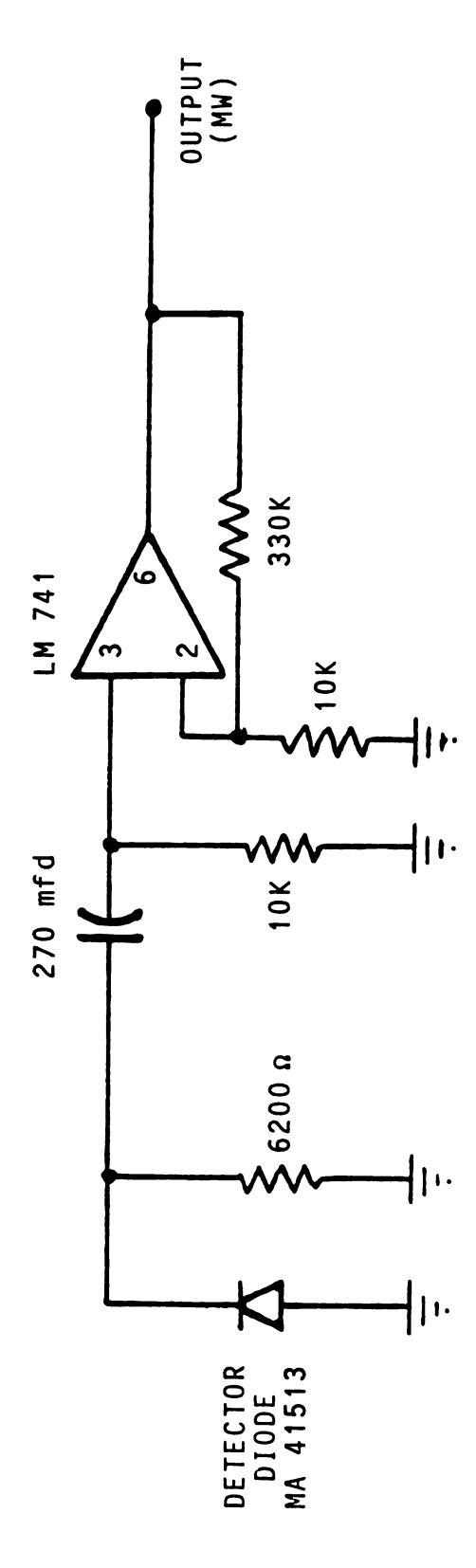


Figure A-5. Schematic Diagram of the Standing Wave Tube Amplifier of the EMT.

APPENDIX B

BASIC ELECTRICAL STRUCTURE OF INTERFACES

Consider a planar interfacial region separating two bulk phases. The direction normal to the interface will be denoted as n, and this is the only direction in which spatial variations can exist. From Maxwell's equations we have:

$$\frac{\partial E}{\partial n} = \rho/\epsilon_0$$
 (Poisson's Law) (B-1)

$$\frac{\partial J}{\partial n} + \partial \rho / \partial t = 0$$
 (Conservation of charge) (B-2)

Here, E is the elctric field intensity, J is the current density, ϵ_0 is the permittivity of free space, and ρ is the charge density contributed by the molecules forming the medium.

Consider first the polarization charges which arise from the orientation of molecular dipoles. It is then correct to write:

$$\rho = \rho_b = -\frac{\partial}{\partial n} P \tag{B-3}$$

where P is the polarization field acting to reduce the electric field within the medium. For a linear dielectric, the polarization is proportional to the electric field:

$$P = \varepsilon_o (\varepsilon - 1) E$$
 (B-4)

where ε is the dielectric constant of the medium and is defined so that when ε = 1, the polarization vanishes and the E field is the same as in free space. Consequently, there results:

$$\frac{\partial}{\partial n} (\varepsilon E) = 0 \tag{B-5}$$

which implies that the product $\varepsilon E = D_o$ where D_o is a displacement field constant everywhere in the two media. Thus:

$$\varepsilon E = D_0$$
 (B-6)

$$\rho = \rho_b = \epsilon_0 D_0 \frac{\partial}{\partial n} \left(\frac{1}{\epsilon} \right) \tag{B-7}$$

These relations show that in bulk phase, E is constant and the polarization charge density is zero. But wherever the dielectric constant varies spatially there is a charge density present.

Consider next the conducted charges which are associated with the finite conductivity of the medium. Ohm's law gives:

$$J_{C} = \sigma E \tag{B-8}$$

Therefore, from (B-1) and (B-2):

$$\sigma \rho_{c}/\varepsilon_{o} + E \frac{\partial \sigma}{\partial n} + \frac{\partial \rho_{c}}{\partial t} = 0$$
 (B-9)

Thus, the conducted charge density will exponentially decay to zero almost instantaneously unless there exists a gradient of the conductivity. A bulk phase will therefore exhibit neither polarization charges nor conduction charges. Spatial inhomogeneities in the conductivity and/or dielectric constant are required for the existence of a non-vanishing charge density.

All media will generally possess both a finite polarizability and conductivity. The above equations then generalize as follows:

$$\frac{\partial}{\partial n} (\sigma E) + \partial \rho_C / \partial t = 0$$
 (B-10)

$$\frac{\partial}{\partial D} (\varepsilon E) = \rho_C / \varepsilon_o$$
 (B-11)

Thus, conduction charges must appear at the interface or else σ and ϵ would have to be proportional everywhere in all media.

When ρ_{C} is eliminated between (B-10) and (B-11), there results:

$$\frac{\partial}{\partial n} \left(\sigma E + \varepsilon_0 \frac{\partial}{\partial t} \left(\varepsilon E \right) \right) = 0$$
 (B-12)

so that everywhere we have:

$$\sigma E + \varepsilon_0 \frac{\partial}{\partial t} (\varepsilon E) = J_0$$
 (B-13)

To first order in spatial variations, (B-13) can be integrated to give:

$$I_o = \frac{V}{R} + \frac{a}{at} (CV)$$
 (B-14)

which is the familiar expression for the total current which flows through a parallel RC circuit when the capacitance is not necessarily constant. Thus, every interface between two media looks electrically like a parallel RC circuit where the resistance is due to conduction charge effects and the capacitance is due to polarization charge effects. These results are illustrated in Figure B-1.

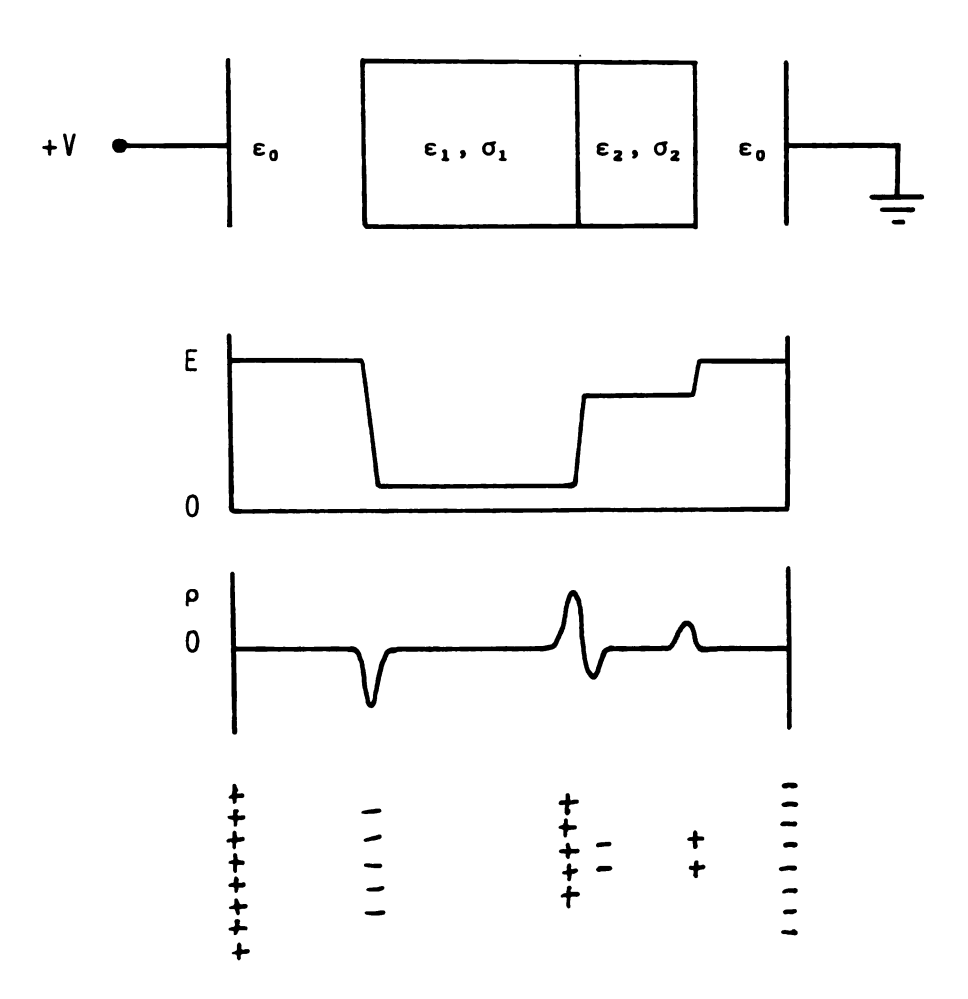


Figure B-1. An Illustration of Electric Field and Charge Distribution at the Interface.

APPENDIX C

AN ELECTROMAGNETIC FORMALISM PERTINENT TO THE ANALYSIS OF MEDIA BY MICROWAVE REFLECTANCE

The Maxwell equations are differential relations between the electric and magnetic fields produced by specified distributions of current and charge densities. As functions of space and time, these read:

$$\nabla \cdot \mathbf{E}(\gamma,t) = \frac{1}{\varepsilon_0} (\gamma,t) \iff \nabla \cdot \mathbf{J}(\gamma,t) + \frac{\partial}{\partial t} (\gamma,t) = 0 \quad (C-1a)$$

$$\nabla \cdot \mathbf{H}(\gamma, t) = 0 \tag{C-1b}$$

$$\nabla \times E(\gamma, t) = - \mu_0 \frac{\partial}{\partial t} H(\gamma, t) \qquad (C-1c)$$

$$\nabla \times \mathbf{H}(\gamma,t) = + \varepsilon_0 \frac{\partial}{\partial t} \mathbf{E}(\gamma,t) + \mathbf{J}(\gamma,t) \qquad (C-1d)$$

The two equations (A-1a) are equivalent because of equation (C-1d). Note that in the absence of sources (i.e., $J(\gamma,t)$ = 0 and $P(\gamma,t)$ = 0) the field exists in free space; consequently, all effects of matter upon the electric and magnetic fields enter the equations through $J(\gamma,t)$ and $P(\gamma,t)$.

The separation-of-variables technique in cartesian coordinates leads to the result that each component of the electric, magnetic, current density, and charge density fields can be written in the form:

$$f(\mathbf{Y},t) = \int \int f(\mathbf{K} \boldsymbol{\omega}) e^{i(\mathbf{K} \cdot \mathbf{Y} + \omega t)} d\mathbf{K} d\boldsymbol{\omega}$$
 (C-2)

Thus, each component of the fields and sources appears as a superposition of harmonic modes with characteristic mode weights which are functions only of a wavevector K and an angular frequency ω . In general, K, ω and f(K, ω) are complex quantities.

Consequently, Maxwell's equations determine the complex mode weights according to the vector algebraic rules:

$$K \cdot E(K, \omega) = -i \frac{1}{\epsilon_0} \rho(K, \omega) \iff K \cdot J(K, \omega) + \omega \rho(K, \omega) = 0 \quad (C-3a)$$

$$\mathbf{K} \cdot \mathbf{H}(\mathbf{K}, \mathbf{\omega}) = 0 \tag{C-3b}$$

$$K \times E(K, \omega) = -\mu_0 \omega H(K, \omega)$$
 (C-3c)

$$\mathbf{K} \times \mathbf{H}(\mathbf{K}, \omega) = +\varepsilon_0 \omega \mathbf{E}(\mathbf{K}, \omega) - i \mathbf{J}(\mathbf{K}, \omega)$$
 (C-3d)

Algebra gives:

$$[\mathbf{K} \cdot \mathbf{K} - \mu_0 \, \varepsilon_0 \, \omega^2] \, \mathbf{E}(\mathbf{K}, \omega) = -i \left[\mu_0 \, \omega \, \mathbf{J}(\mathbf{K}, \omega) + \frac{1}{\varepsilon_0} \, \rho(\mathbf{K}, \omega) \right] \tag{C-4a}$$

$$[K \cdot K - \mu_0 \varepsilon_0 \omega^2] H(K, \omega) = +i[K \times J(K, \omega)]$$
 (C-4b)

As a result of the above manipulations, when $J(\gamma,t)$ and $\rho(\gamma,t)$ are known in the form:

$$\rho(\gamma,t) = \int \int \rho(K,\omega) e^{i(K \cdot \gamma + \omega t)} dK d\omega \qquad (C-5a)$$

$$J(\gamma,t) = \int \int J(K,\omega) e^{i(K\cdot\gamma + \omega t)} dK d\omega \qquad (C-5b)$$

then $E(\gamma,t)$ and $H(\gamma,t)$ are specified:

$$E(\gamma,t) = \int \int E(K,\omega) e^{i(K \cdot \gamma + \omega t)} dK d\omega \qquad (C-6a)$$

$$H(\gamma,t) = \int \int H(K,\omega) e^{i(K \cdot \gamma + \omega t)} dK d\omega$$
 (C-6b)

where $E(K,\omega)$ and $H(K,\omega)$ are given by (C-4a) and $\overline{\ }$ (C-4b) above.

For typographical convenience and clarity, the arguments of space and time dependent quantities will be given explicitly, whereas the arguments of quantities dependent upon K and ω will be deleted. Thus, $A(K,\omega)$ will be denoted simply as A. Consequently, the mode amplitudes are prescribed by:

$$\mathbf{K} \cdot \mathbf{E} = -i \ \rho/\varepsilon_0 \iff \mathbf{K} \cdot \mathbf{J} + \omega \rho = 0$$
 (C-7a)

$$\mathbf{K} \cdot \mathbf{H} = 0 \tag{C-7b}$$

$$K \times E = -\mu_0 \omega H \qquad (C-7c)$$

$$\mathbf{K} \times \mathbf{H} = +\mu_0 \, \omega \mathbf{E} - \mathbf{i} \, \mathbf{J} \tag{C-7d}$$

$$[K \cdot K - \mu_0 \varepsilon_0 \omega^2]E = -i[\mu_0 \omega J + \frac{1}{\varepsilon_0} \rho] \qquad (C-8a)$$

$$[K \cdot K - \mu_0 \varepsilon_0 \omega^2]H = +i[K \times J] \qquad (C-8b)$$

In the following development, certain combinations of E, H, J and ρ play a major role. These are denoted as follows:

$$Q \equiv E \cdot J$$

complex power density

$$L \equiv \mu_0 H \cdot H - \epsilon_0 E \cdot E$$

 $L \equiv \mu_0$ $H \cdot H - \epsilon_0 E \cdot E$ complex Lagrangian density

complex energy flux

$$F \equiv \rho E + \mu_0 J \times H$$

 $\mathbf{F} \equiv \rho \mathbf{E} + \mu_0 \mathbf{J} \times \mathbf{H}$ complex force density

Note that the above complex quadratic quantities are similar in form to the real (space and time dependent) power density, Langrangian density, Poynting vector, and Lorentz force density, respectively. However, the above quantities are in fact the generalized Fourier transforms of convolutions over the respective space and time dependent quantities according to the theorems:

$$\frac{1}{(2\pi)^4} \left[\int \int A(\gamma',t') B(\gamma-\gamma',t-t') d\gamma'dt' \right] e^{-i(K\cdot\gamma+\omega t)} d\gamma dt$$

$$= A(K,\omega) B(K,\omega) \qquad (C-9a)$$

Consequently, the simple manipulations in K, w space which follow represent very complicated relationships between the corresponding quantities in real space and However, the goal of the following derivation is a dispersion relation in K, ω space, whereas the corresponding relations in real space and time are of lesser importance

at present. Systematic scalar multiplication (i.e., formation of dot products) of equations (C-7) by \mathbf{E} , \mathbf{H} , and \mathbf{J} yields:

$$\mathbf{E} \cdot \mathbf{H} = \mathbf{E} \cdot \mathbf{S} = \mathbf{H} \cdot \mathbf{S} = 0 \tag{C-10}$$

$$K \cdot H = J \cdot H = F \cdot H = 0 \tag{C-11}$$

Therefore, the complex vectors E, H, and S form an orthogonal triad in K, ω space, and the vectors K, J, and F lie perpendicular to H (i.e., in the E,S plane). Scalar multiplication also reveals that:

$$K \cdot S = iQ - \omega \varepsilon_0 E \cdot E = -\omega \mu_0 H \cdot H$$
 (C-12)

so that:

$$Q = i\omega L = i\omega (\mu_0 H \cdot H - \epsilon_0 E \cdot E) \qquad (C-13)$$

Cross multiplication of (C-7b) by E gives:

$$i \mathbf{J} \times \mathbf{E} = i \rho/\epsilon_0 \mathbf{H} = \mathbf{K} \times \mathbf{S}$$
 (C-14)

Finally, crossing (C-7c) with \mathbf{E} , and (A-7d) with \mathbf{H} yields:

$$-\mu_0 \, \epsilon_0 \, S = K \epsilon_0 E \cdot E + i \, \rho / \epsilon_0 = K \mu_0 \, H \cdot H \, - i \, \mu_0 \, J \times H \qquad (C-15)$$

so that the important result is derived:

$$\mathbf{F} = -i \, \mathsf{L} \, \mathsf{K} = - \, \frac{\mathsf{Q}}{\mathsf{\omega}} \, \, \mathsf{K} \tag{C-16}$$

As a result of the above, the geometry of the complex field vectors in $\mathbf{K}, \boldsymbol{\omega}$ space can be sketched to illustrate the following important points:

- (a) K, J, and F lie in the E, S plane and are always perpendicular to H.
- (b) When $\rho=0$ and J=0, the force density vanishes, and K is parallel to S.
- (c) When $\rho = 0$ and $\mathbf{J} \neq 0$, both the force density and K are parallel to S, and J is parallel to E.
- (d) When $\rho \neq 0$ and J=0, the field is electrostatic and H=0. In this case, K and F are parallel to E, and S=0.
- (e) When $\rho \neq 0$ and $J \neq 0$, K is not parallel to S, and J is not parallel to E.
- (f) In all cases, F is parallel to K.
 For present purposes, attention will be restricted to two cases only:
 - (i) $\rho=0$ and $J\neq0$ so that J is parallel to E. In such a case, the most general allowed relation between J and E is $J=\sigma E$, where σ is the complex conductivity. Such a medium obeys Ohm's law and is called "Ohmic." From (C-14), we find that $J=\sigma E$ implies $\rho=0$ and that $\rho=0$ implies $J=\sigma E$.
- (ii) $_{\rho} \neq 0$ and J $\neq 0$ so that J cannot be parallel to E but must still lie in the E,S plane. In such a case, the most general allowed relation between J and E is $J = E + \frac{1}{\Phi} S$, where Φ is a complex potential. Such a

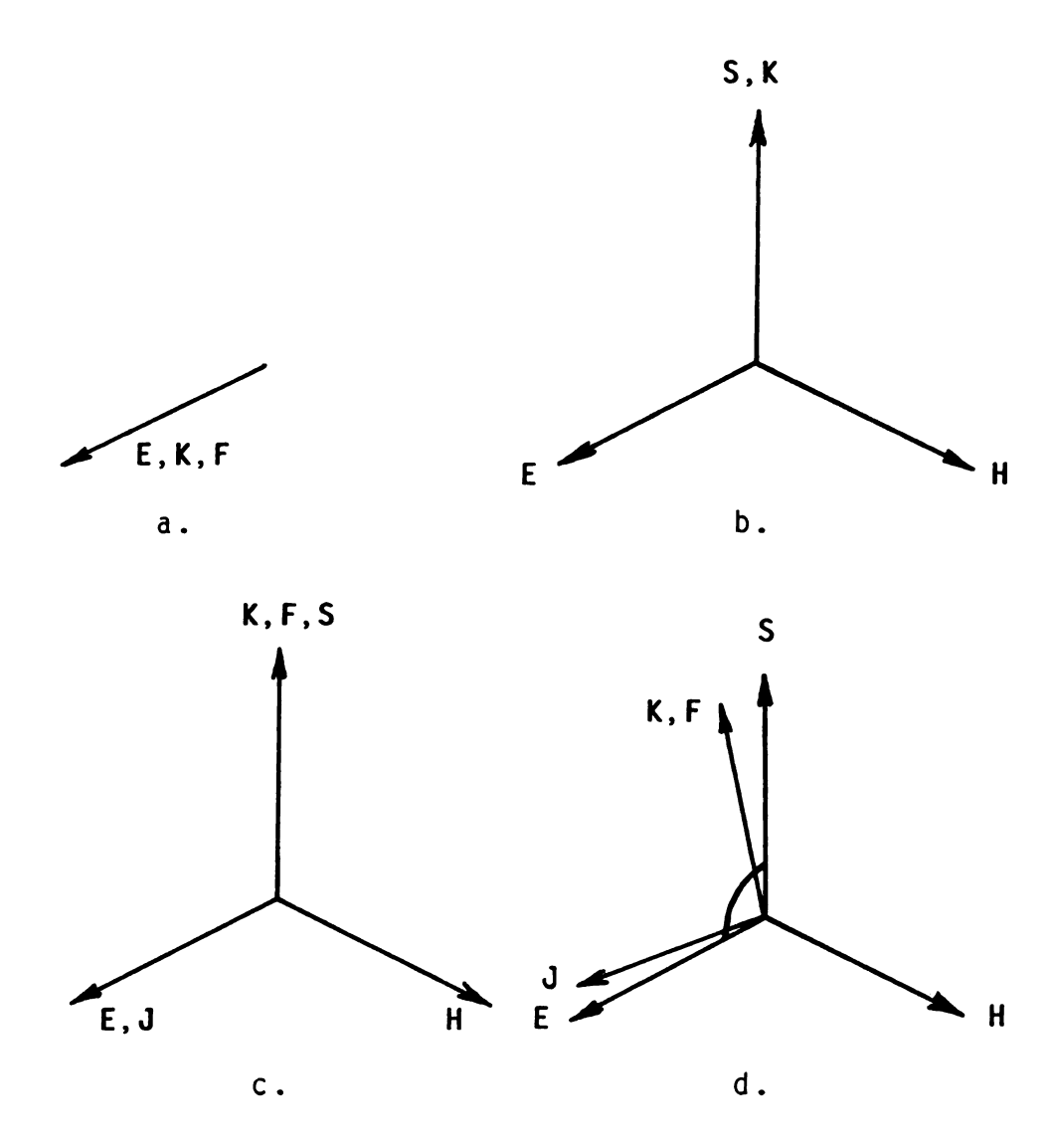


Figure C-1. Complex field configurations in K, space.

- $\rho \neq 0, J = 0$ $\rho = 0, J = 0$ $\rho = 0, J \neq 0$ $\rho \neq 0, J \neq 0$
- b.)
 c.)
 d.)

These special cases are named as follows: (a) electrostatic; (b) free-space; (c) Ohmic; and (d) non-Ohmic.

medium will be called "non-Ohmic," because in addition to the Ohmic current, there also exists a drift current (Hall current) in the direction of S.

Note that in either case, $Q \equiv E \cdot J \equiv \sigma E \cdot E$. Also, from (C-14) there follows:

$$\Phi_{\rho} = \varepsilon_0 \mathbf{E} \cdot \mathbf{E} \tag{C-17}$$

Consequently, the most general relation between ${\bf J}$ and ${\bf E}$ can be written as:

$$\mathbf{J} = \sigma[\mathbf{E} + \frac{\rho}{\epsilon_0} \frac{1}{\mathbf{Q}} \mathbf{S}] \tag{C-18}$$

which correctly reduces to 0hm's law when $\rho = 0$.

At this point in the development, we return to equations (C-8) and find by scalar multiplication:

$$(\mathbf{K} \cdot \mathbf{K} - \mu_0 \, \epsilon_0 \, \omega^2) \, \epsilon_0 \, \mathbf{E} \cdot \mathbf{E} = -i \, \epsilon_0 \, \mu_0 \, \omega Q - \frac{1}{\epsilon_0} \, \rho^2 \qquad (C-19a)$$

$$(\mathbf{K} \cdot \mathbf{K} - \mu_0 \, \varepsilon_0 \, \omega^2) \, Q = -i \, \omega (\mu_0 \, \mathbf{J} \cdot \mathbf{J} - \frac{1}{\varepsilon_0} \, \rho^2)$$
 (C-19b)

$$(\mathbf{K} \cdot \mathbf{K} - \mu_0 \, \epsilon_0 \, \omega^2) \, \mu_0 \, \mathbf{H} \cdot \mathbf{H} = -i \, \epsilon_0 \, \mu_0 \, \omega \mathbf{Q} - \mu_0 \, \mathbf{J} \cdot \mathbf{J}$$
 (C-19c)

For present purposes, (C-19a) is most convenient for obtaining the desired dispersion relation. Dividing by ϵ_n E•E gives:

$$\mathbf{K} \cdot \mathbf{K} = \mu_0 \, \epsilon_0 \, \omega^2 - i \, \mu_0 \, \omega \sigma - \frac{\rho^2}{\epsilon_0} \left[\epsilon_0 \, \mathbf{E} \cdot \mathbf{E} \right]^{-1}$$
 (C-20)

which can also be written:

$$\mathbf{K} \cdot \mathbf{K} = \mu_0 \, \varepsilon_0 \, \omega^2 - i \, \mu_0 \, \omega \sigma \left[1 - \frac{i}{\mu_0 \, \varepsilon_0 \, \omega^2} \, \frac{\rho^2}{\varepsilon_0} \, \frac{\omega}{Q} \right] \tag{C-21}$$

Finally, use of (C-19b) to eliminate Q gives:

$$K \cdot K = \mu_0 \varepsilon_0 \omega^2 - i \mu_0 \omega \sigma \left[\frac{\mu_0 \mathbf{J} \cdot \mathbf{J} - \frac{1}{\varepsilon_0} \rho^2}{\mu_0 \mathbf{J} \cdot \mathbf{J} - \frac{1}{\varepsilon_0} \rho^2 (1 - \frac{i \sigma}{\varepsilon_0 \omega})} \right] \qquad (C-22)$$

Note that (C-21) and/or (C-22) show that when $\sigma=0$, there results the free space dispersion relation, since in this case, ${\bf J}=0$ by (C-18) and hence also $\rho=0$ by (C-7a). When $\sigma\neq 0$ but $\rho=0$, there results the Ohmic dispersion relation:

$$\mathbf{K} \cdot \mathbf{K} = \mu_0 \, \varepsilon_0 \, \omega^2 - i \, \mu \omega \, \sigma \tag{C-23}$$

The Ohmic dispersion is independent of the field strength. The dispersion relation of a non-Ohmic medium (i.e., $\rho \neq 0$) is, however, manifestly field strength dependent. This dependence can be expressed in terms of ρ and one other parameter (either $\mathbf{E} \cdot \mathbf{E}$, $\mathbf{E} \cdot \mathbf{J}$, or $\mathbf{J} \cdot \mathbf{J}$ in (C-20), (C-21), or (C-22), respectively). Equations (C-21) and (C-22) show that this field strength dependence is formally equivalent to introducing a field strength dependence in the conductivity. For a medium characterized by potential variations (e.g., neural tissue), a convenient dispersion relation is:

$$\mathbf{K} \cdot \mathbf{K} = \mu_0 \, \varepsilon_0 \, \omega^2 - i \, \mu \omega \sigma - \frac{\rho}{\varepsilon_0} \, \frac{1}{\Phi}$$
 (C-24)

where Φ is defined in (C-17). Note that no divergence occurs as $\Phi \to 0$, since by (C-17) and (C-7a) this condition is equivalent to $\rho \to 0$.

At this point, it is pertinent to demonstrate that a necessary and sufficient condition for a medium to be non-Ohmic and hence to possess a field dependent dispersion relation is that the measurable conductivity be a tensor of rank higher than zero (i.e., have direction dependence). That is, if we write:

$$\mathbf{J} = \underline{\sigma} \cdot \mathbf{E} \tag{C-25}$$

where $\underline{\bullet}$ is a matrix which is not a scalar multiple of the unit matrix, then J will not be parallel to E, and by (C-14), ρ will not vanish. Conversely, if the medium is non-Ohmic, then by definition, ρ is non-zero and J is not parallel to E, i.e., the conductivity has tensor character. As a corollary, all systems composed of interfaces (membranes) are somewhat non-Ohmic, since the measurable conductivity is different across and along the interface. Consequently, as is well known, all interfaces possess some degree of non-vanishing charge density with concommitant non-Ohmic behavior.

The formulas developed in this section are applied in the following Appendices.

APPENDIX D

MICROWAVE REFLECTANCE FROM OHMIC MEDIA

In general, $E(\gamma,t)$ and $H(\gamma,t)$ must have continuous components tangential to any interface. This requirement leads directly to the result that the interface will yield a reflected field related to the incident field as:

$$E(\gamma,t)_{refl} = R E(\gamma,t)_{inc}$$
 (D-1)

where the complex reflection coefficient has the form:

$$R = \frac{K - K'}{K + K'} \tag{D-2}$$

where K is the wavevector in the medium supporting the incident and reflected fields, and K' is the wavevector in the medium supporting the transmitted fields. Note that the reflected field vanishes when K = K', i.e., when the interface vanishes.

It is precisely because the reflection coefficient depends on the dispersion relations in the adjoining media only, and not explicitly on the field magnitudes, that so much attention was devoted to developing dispersion relations in Appendix C.

For the remainder of the present section, the following conditions are assumed:

(a) The reflected and transmitted waves are of the transverse electromagnetic type in a medium behaving as free space. Such a condition is met when a lossless section of coaxial cable is operated in the dominant mode and is terminated by a free end (i.e., probe tip) cut transversely to the axis.

- (b) The transmitted wave is supported by an Ohmic medium (i.e., $J(K,\omega) = \sigma(K,\omega) E(K,\omega)$).
- (c) The probe tip is in perfect contact with the Ohmic medium.

Consequently, by (C-23), we have the dispersion relations:

$$\mathbf{K} \cdot \mathbf{K} = \mu_0 \, \epsilon_0 \, \omega^2$$
 Inside coax (D-3a)

$$K' \cdot K' = \mu_0 \epsilon_0 \omega^2 - i \mu_0 \omega \sigma$$
 inside Ohmic medium (D-3b)

In the present case, **K** has only one component which will be denoted K and is measured along the axis. Also, **K'** has but one component at the interface, which is parallel to **K** and will be denoted K'. Both K and K' are complex. Consequently, combining (D-3a) and (D-3b) gives:

$$K^{1^2} = K^2 - i \mu_0 \omega \sigma \qquad (D-4)$$

so that the following is obtained:

$$R = \frac{1 - K'/K}{1 + K'/K} ; \quad \left(\frac{K'}{K}\right)^2 = 1 - i \frac{\sigma}{\varepsilon_0 \omega}$$
 (D-5)

Equations (D-5) provide a complete description of the Ohmic reflectance. Note that R is independent of field strength. This means that reflectance from an Ohmic medium (physiological saline, for example) will never reveal the

existence of externally applied currents flowing by volume conduction through the medium. Such currents may be detectable, however, when the applied voltage is sufficient to cause electrolysis, since in this case the medium contains free charges and is no longer Ohmic. Of course, the reflectance will change when σ is varied, for example, by chemical means or by varying the temperature.

The experiments described in this thesis make no direct use of the temporal phase information contained in the complex reflection coefficient, i.e., the magnitude alone is monitored. Before deriving the form of this magnitude, it is convenient to make the substitution:

$$\sigma = \sigma_r + i\sigma_i = \sigma_r + i(\varepsilon_r - 1)\varepsilon_\sigma \omega$$
 (D-6)

so that (B-3b) assumes the standard form:

$$K^{12} = \mu_0 \varepsilon_0 \omega^2 \varepsilon_{\Gamma} - i \mu_0 \omega \sigma_{\Gamma} \qquad (D-7)$$

where $\epsilon=1-\sigma_i/\epsilon_o\,\omega$ is the real dielectric constant, and σ_r is the real conductivity. Then:

$$R = \frac{1 - K'/K}{1 + K'/K} ; \qquad (\frac{K'}{K})^2 = \epsilon_r - i \frac{\sigma_r}{\epsilon_0 \omega}$$
 (D-8)

Letting $R = R_r + iR_i$ and separating real and imaginary parts gives:

$$R = \frac{1 - c^2 - d^2}{(1+c)^2 + d^2}$$
 (D-9a)

$$R = \frac{-2d}{(1+c)^2 + d^2}$$
 (D-9b)

where c^z - d^z = ε_r and 2cd = $-\sigma_r \, / \, \varepsilon_o \, \, \omega$ so that there results:

$$c^2 = \frac{1}{2} \left[\sqrt{a^2 + b^2} + a \right]$$
 (D-10a)

$$d^2 = \frac{1}{2} \left[\sqrt{a^2 + b^2} - a \right]$$
 (D-10b)

where $a = \epsilon_r$ and $b = \sigma_r / \epsilon_o \omega$. Finally:

$$R_r = \frac{1 - \sqrt{a^2 + b^2}}{1 + \sqrt{a^2 + b^2} + \sqrt{2} \sqrt{\sqrt{a^2 + b^2} + a}}$$
 (D-11a)

$$R_{i} = \frac{-\sqrt{2} \sqrt{\sqrt{a^{2} + b^{2}} - a}}{1 + \sqrt{a^{2} + b^{2}} + \sqrt{2} \sqrt{\sqrt{a^{2} + b^{2}} + a}}$$
 (D-11b)

$$|R|^2 = R_r^2 + R_i^2$$
 (D-12)

In general, no simplifying approximations are possible when X-band radiation is used since in this case $\epsilon_o \; \omega \; \approx \; \% (\text{MKS units}), \; \text{and for physiological systems,} \; \epsilon_r \; \text{and} \; \sigma_r$ may have comparable numerical values.

APPENDIX E

MICROWAVE REFLECTANCE FROM NON-OHMIC MEDIA

Whereas the dispersion relation, and hence the reflection coefficient, of an Ohmic medium depends on a single constitutive parameter (i.e., the complex conductivity σ), the dispersion relation and reflection coefficient of a non-Ohmic medium depends upon the conductivity (σ), the charge density (ρ), and one field intensity (either E or J). Consequently, the non-Ohmic dispersion is specified uniquely only when the details of the system and the means used to measure the reflection coefficient are specified. For the remainder of the present section, the following

(a) The reflected and incident fields are of the transverse electromagnetic type in a medium behaving as free space (i.e., transversely cut end of a lossless coaxial cable).

conditions are assumed:

- (b) The transmitted fields are supported by a non-Ohmic medium (i.e., $\rho \neq 0$).
- (c) The probe tip is in perfect contact with the medium.

In general, a non-Ohmic medium will be embedded in an Ohmic medium. For example, the free charge in a partially ionized gas is embedded in a neutral gas medium; the free charge forming the electrical double layers of living cell membranes exists against a saline medium. Thus, the reflection coefficient will have the same form as (D-2)

but will depend upon the non-Ohmic dispersion relation. Consider the following dispersion relations:

$$K^2 = \mu_0 \epsilon_0 \omega^2$$
 (free space) (E-1a)

$$K^{12} = \mu_0 \varepsilon_0 \omega^2 - i \mu_0 \omega \sigma \qquad (Ohmic) \qquad (E-1b)$$

$$K^{112} = \mu_0 \, \epsilon_0 \, \omega^2 - i \, \mu_0 \, \omega \sigma - \frac{\rho^2}{\epsilon_0} \, \frac{1}{\epsilon_0 \, E \cdot E} \qquad (\text{non-Ohmic}) \qquad (E-1c)$$

Consequently, there results:

$$R = \frac{1 - \frac{K}{K}}{1 + \frac{K}{K}}; \quad (\frac{K''}{K})^2 = 1 - i \frac{\sigma}{\varepsilon_0 \omega} - \frac{1}{\mu_0 \varepsilon_0 \omega^2} \frac{\rho^2}{\varepsilon_0} \frac{1}{\varepsilon_0 E \cdot E}$$
 (E-2)

If the relation $Q = \sigma E \cdot E$ is inserted in (E-2), a simplification results:

$$\left(\frac{K''}{K''}\right)^2 = 1 - \frac{i\sigma}{\varepsilon_0 \omega} \left[1 - \frac{i}{\mu_0 \varepsilon_0 \omega^2} \frac{\rho^2}{\varepsilon_0} \frac{\omega}{Q}\right]$$
 (E-3)

so that the formulas of Appendix D become applicable to the non-Ohmic case when the following substitution is made:

$$\sigma \to \sigma \left[1 - \frac{i}{\mu_0 \, \epsilon_0 \, \omega^2} \, \frac{\rho^2}{\epsilon_0} \, \frac{\omega}{Q}\right] \tag{E-4}$$

In order to proceed further, specific non-Ohmic systems must be examined. The first, and simplest, such system to be considered is the partially ionized gas. Microwave reflectance is a well-known tool in the field of plasma diagnostics, and various types of glow discharge tubes are used in the calibration of the microwave devices

used in biophysical investigations (especially the Standing Wave Tube and Electromagnetrode). A general discussion of non-Ohmic plasma behavior is therefore pertinent to the present exposition. For simplicity, a one-fluid model will be adopted.

Before the electromagnetic formalism of Appendix C can be applied to a plasma, a momentum transport equation, consistent with Maxwell's equations, must be proposed. Logically, this is because Maxwell's equations describe the behavior of the electromagnetic field for prescribed source distributions, and the momentum equation describes the behavior of the sources in the presence of an electromagnetic field; thus, a close system of equations results. In real space and time, we have the Langevin equation:

$$\frac{d}{dt} P(\gamma,t) + \nu P(\gamma,t) = \rho(\gamma,t) E(\gamma,t) +$$

$$\mu_0 J(\gamma,t) \times H(\gamma,t)$$
(E-5)

where $P(\gamma,t)$ is the momentum density, and ν is a phenomenological damping frequency. The momentum density can be written:

$$P(\gamma,t) = m(\gamma,t) V(\gamma,t)$$
 (E-6)

where $V(\gamma,t)$ is a velocity field of the kind studied in fluid dynamics. The mass density $m(\gamma,t)$ is proportional to the charge density $\rho(\gamma,t)$ by the factor ξ , which is the charge to mass ratio of the particles comprising the

fluid plasma:

$$\xi = \frac{\rho(\Upsilon, t)}{m(\Upsilon, t)} = \frac{Q_o}{m_o} = constant$$
 (E-7)

Consequently, (E-6) is equivalent to:

$$J(\gamma,t) = \rho(\gamma,t) \quad V(\gamma,t)$$
 (E-8)

where $J(\gamma,t)$ and $\rho(\gamma,t)$ are related by (C-1a). Thus, Maxwell's equations require conservation of charge, and this, by (E-7), requires a conservation of mass:

$$\frac{\partial}{\partial t} \rho(\mathbf{\gamma}, t) + \nabla \cdot \mathbf{J}(\mathbf{\gamma}, t) = 0 = \frac{d}{dt} m(\mathbf{\gamma}, t) + \nabla \cdot \mathbf{P}(\mathbf{\gamma}, t)$$
 (E-9)

Mass conservation allows the total derivative of momentum density in (E-5) to be evaluated using a lengthy sequence of standard vector calculus operations:

$$\frac{d}{dt} = P(\gamma, t) = m(\gamma, t) \frac{d}{dt} V(\gamma, t)$$
 (E-10)

$$\frac{d}{dt} V(\gamma, t) = \frac{\partial}{\partial t} V(\gamma, t) + V(\gamma, t) \cdot \nabla V(\gamma, t) \qquad (E-11)$$

$$V(\gamma,t) \cdot \nabla V(\gamma,t) = \frac{1}{2}\nabla(V(\gamma,t) \cdot V(\gamma,t)) + \Omega(\gamma,t) \times V(\gamma,t)$$
 (E-12)

where the vector symbol $\Omega(\Upsilon,t) \equiv \nabla \times V(\Upsilon,t)$ has been used for the fluid rotation.

Combining (E-10), (E-11), and (E-12) gives:

$$\frac{d}{dt} P(\gamma, t) = m(\gamma, t) \frac{\partial}{\partial t} V(\gamma, t) + \frac{1}{2}m(\gamma, t) \nabla(V(\gamma, t) \cdot V(\gamma, t))$$

$$+ \Omega(\gamma, t) \times P(\gamma, t) \qquad (E-13)$$

which can be written:

$$\frac{d}{dt} P(\gamma,t) = \frac{\partial}{\partial t} P(\gamma,t) + \Omega(\gamma,t) \times P(\gamma,t) + \nabla p(\gamma,t) - (E-14)$$

$$P(\gamma,t) \frac{1}{m(\gamma,t)} \frac{\partial}{\partial t} m(\gamma,t) - p(\gamma,t) \frac{1}{m(\gamma,t)} \nabla m(\gamma,t)$$

where $p(\gamma,t) \equiv \frac{1}{2}m(\gamma,t)$ $V(\gamma,t) \cdot V(\gamma,t)$ is the kinetic energy density or pressure. The total derivative of the momentum density is thus:

$$\frac{d}{dt} P(\gamma, t) = \frac{\partial}{\partial t} P(\gamma, t) + \Omega(\gamma, t) \times P(\gamma, t) + \nabla p(\gamma, t) \qquad (E-15)$$

where the last two terms on the right hand side of (E-14) have been neglected since they are proportional to the temporal and spatial rates of change of the logarithm of the mass density, which are always much smaller than the temporal and spatial rates of change of the mass density proper. Consequently, a one-fluid Langevin equation consistent with Maxwell's eugations is:

$$\frac{\partial}{\partial t} \mathbf{J}(\gamma, t) + \mathbf{v} \mathbf{J}(\gamma, t) + \Omega(\gamma, t) \times \mathbf{J}(\gamma, t)$$
 (E-16)

=
$$\xi[\rho(\gamma,t) E(\gamma,t) + \mu_0 J(\gamma,t) \times H(\gamma,t) - \nabla p(\gamma,t)]$$

where the relation $\xi P(\gamma,t) = J(\gamma,t)$ has been used. Equation (E-16) can be transformed to K,ω space using (C-2) and (C-9b):

$$(i\omega + v) \ J(K, \omega) + i \xi p(K, \omega) K$$
 (E-17)
$$= \iint \xi p(K', \omega') \ E(K - K', \omega - \omega') + J(K', \omega') \times$$
 [\Omega(K - K', \omega - \omega') + \mu_0 \xi H(K - K', \omega - \omega')] \, dK' \, d\omega' \)

Equation (E-17) is obviously quite complicated and shows, among other things, that the various harmonic modes of the current density tend to be coupled by convolution integrals so that momentum can be exchanged between modes in an infinite variety of ways. Thus, although the plasma currents must be continuous with continuous first derivatives, the plasma is inherently unstable in the general case and exhibits a marked tendency toward turbulent behavior (e.g., the flickering of flames, flourescent tubes, etc.). The sifting property of the delta function allows (E-17) to be written as the momentum transfer selection rule:

The principal utility of equation (E-18) is that a selection rule for the complex power density can be obtained by scalar multiplication by $J(K',\omega')$:

In the simplest case, a single K and ω are allowed so the plasma sustains monochromatic oscillations. Then $E(K-K',\omega-\omega')=E(K',\omega')\;\delta(K-K',\omega-\omega'),\;\text{and}\;(E-19)$ simplifies to:

$$(i\omega + v)$$
 $\mathbf{J} \cdot \mathbf{J} = Q\xi\rho + i\rho\xi\omega\rho$ (E-20)

where the (K,ω) arguments have been suppressed as in Appendix C and relation (C-7a) has been used. Substitution in (C-19b) gives:

$$\mathbf{K} \cdot \mathbf{K} - \mu_0 \, \varepsilon_0 \, \omega^2 = -i \mu_0 \, \xi \rho \frac{\mathbf{J} \cdot \mathbf{J} - \frac{1}{\mu_0 \, \varepsilon_0} \, \rho^2}{(i + \frac{\nu}{\omega}) \, \mathbf{J} \cdot \mathbf{J} - i \, \xi \rho \rho}$$
 (E-21)

which can be simplified using (C-22) to eliminate ${f J}$. ${f J}$.

Algebraic manipulation yields a "warm plasma" dispersion relation:

$$\begin{split} &i\,\mu_{0}\,\xi\,\rho\big[\rho\,(\,\textbf{K}\,\boldsymbol{\cdot}\,\textbf{K}\,\,-\,\,\mu_{0}\,\,\varepsilon_{0}\,\,\omega^{2})\,\,+\,\frac{\rho^{2}}{\varepsilon_{0}}\big]\big[\,\textbf{K}\,\boldsymbol{\cdot}\,\,\textbf{K}\,\,-\,\,\mu_{0}\,\,\varepsilon_{0}\,\,\omega^{2}\,\,+\,\,i\,\mu_{0}\,\,\omega\sigma\,\big] \\ &=\,\frac{\rho^{2}}{\varepsilon_{0}}\big[\,(\,1\,\,\frac{\,\mathrm{i}\,\sigma}{\varepsilon_{0}\,\,\omega})\,\,\,\textbf{K}\,\boldsymbol{\cdot}\,\textbf{K}\,\,-\,\,\mu_{0}\,\,\varepsilon_{0}\,\omega^{2}\big]\big[\,(\,i\,\,+\,\,\frac{\nu}{\omega})\,(\,\textbf{K}\,\boldsymbol{\cdot}\,\textbf{K}\,\,-\,\,\mu_{0}\,\,\varepsilon_{0}\,\omega^{2})\,\,+\,\,i\,\mu_{0}\,\,\xi\rho\,\big] \end{split} \tag{E-22}$$

This relation is quadratic in $K \cdot K$, but simplifies in the "cold plasma" approximation, i.e., when p and v are zero. Such a case corresponds to sufficiently low density such that collisions are negligible and the plasma is driven in synchrony with the fields. In this case, we have:

$$i \omega \mathbf{J} \cdot \mathbf{J} + Q \xi \rho$$
 (E-23)

$$K \cdot K - \mu_0 \varepsilon_0 \omega^2 = -\mu_0 \xi \rho + \frac{\rho^2}{\varepsilon_0} \frac{\xi \rho}{J \cdot J}$$
 (E-24)

$$\mathbf{K} \cdot \mathbf{K} - \mu_0 \, \varepsilon_0 \, \omega^2 = -i \, \mu_0 \, \omega \sigma \left[1 - \frac{i}{\mu_0 \, \varepsilon_0 \, \omega^2} \, \frac{\rho^2}{\varepsilon_0} \, \frac{\omega}{Q} \right] \tag{E-25}$$

where (E-23) and (E-24) are obtained from (E-20) and (E-21) respectively, and (E-25) is the same as (C-21). Taken together, these give:

$$\mathbf{K} \cdot \mathbf{K} - \mu_0 \, \varepsilon_0 \, \omega^2 = -i \, \mu_0 \, \omega \sigma \left[\frac{1 - \frac{\xi \rho}{\varepsilon_0 \, \omega^2}}{1 - i \frac{\sigma}{\varepsilon_0 \, \omega}} \right] \tag{E-26}$$

Equation (E-26) is the non-Ohmic dispersion relation for a medium characterized by a complex conductivity σ and a free charge density of sufficiently small magnitude that thermal gradients are unimportant. Although the derivation

leading to (E-26) above is long and involved, the result (E-26) follows directly from (C-19a) and (C-19b) when the Langvin equation is used in its K,ω space representation. A less rigorous derivation is also possible by simply postulating a K,ω space force equation:

$$F = i_{\omega}P + i_{\omega} \times P \qquad (E-27)$$

which is the "cold" analogue of (E-18). Then using $\xi P = J$ and (C-16), we have directly:

$$-\frac{Q}{\omega}\xi K = i\omega J + i\omega \times J \qquad (E-28)$$

which gives (E-23) immediately when dot multiplied by **J**. Although (E-27) is simply postulated as a plausible force equation, it is based on the Langevin equation which is also postulated. Either way, one still obtains the non-Ohmic dispersion (E-26). Note that the quantity $(\frac{1}{\epsilon_0}\xi_P)^{\frac{1}{2}}$ is the plasma angular frequency, so:

$$\omega_{\rho}^{2} \equiv \frac{1}{\varepsilon_{0}} \xi \rho$$
 (E-27)

$$\mathbf{K} \cdot \mathbf{K} = \mu_0 \, \varepsilon_0 \, \omega^2 - i \, \mu_0 \, \omega \, \sigma \left[\frac{1 - \left(\frac{\omega \, p}{\omega}\right)^2}{1 - i \, \frac{\sigma}{\varepsilon_0 \, \omega}} \right] \tag{E-28}$$

Thus, for example, microwave reflectance can be observed for neon glow discharges, and this reflectance can be modulated by variation of ω_p^2 which is directly proportional to the charge density. Such density variations can be produced by application of an external electric field

(for example, at audio frequencies so that (E-28) indicates that the microwave reflectance will be modulated at the corresponding audio frequency). Such "intermodulation" is not possible without a non-Ohmic dispersion relation.

At this point, we may consider a non-Ohmic model of nerve tissue in order to demonstrate the possibility of modulation of microwave reflectance by neural activity, i.e., depolarization of neural membranes. The primary distinction between the non-Ohmic response of a plasma and that of neural tissue is that the charge density within neural tissue is bound to the membrane in various ways. Bound charges and their associated currents can be described in coordinate space and time as:

$$\rho_{b}(\gamma,t) = - \nabla \cdot P(\gamma,t) \qquad (E-29a)$$

$$\mathbf{J}_{b}(\gamma,t) = +\frac{\partial}{\partial t} P(\gamma,t) \qquad (E-29b)$$

where $P(\gamma,t)$ is the polarization field. Fourier transformation gives:

$$\rho_b = -i K \cdot P \qquad (E-30a)$$

$$\mathbf{J}_{b} = +i \,\omega \,\mathbf{P} \tag{E-30b}$$

Consequently, the description of a non-Ohmic medium consisting of polarization charges within a medium of finite conductivity is given by:

$$(K^{2} - \mu_{0} \varepsilon_{0} \omega^{2}) E = -i (\mu_{0} \omega J + \frac{\rho}{\varepsilon_{0}} K) \qquad (E-31)$$

$$\rho = -i K \cdot P \qquad (E-32a)$$

$$\mathbf{J} = \sigma \mathbf{E} + i \omega \mathbf{P} \tag{E-32b}$$

Now since $J \cdot H = 0$ and $E \cdot H = 0$, it follows that P must lie in the E,S plane as described in Appendix C. Therefore, we can write:

$$P = P_{E} + P_{S} \tag{E-33}$$

where $P_{\xi} \cdot P_{\zeta} = 0$. For a linear material, the polarization in the direction of E can be written:

$$P_{r} = \varepsilon_{o} (\varepsilon - 1) E \qquad (E-34)$$

so that we have:

$$\mathbf{J} = [\sigma + \varepsilon_0 (\varepsilon - 1) i\omega] \mathbf{E} + i\omega \mathbf{P}_S$$
 (E-35)

Consequently, the polarization field parallel to E does not contribute to a charge density as seen by the field, for if $P_S=0$, then J is parallel to E and $\rho=0$ by (C-14). The effects of P_E are embodied in the dielectric constant ϵ . (E-31) becomes:

$$(K' - \mu_0 \varepsilon_0 \omega^2 \varepsilon + i \mu_0 \omega\sigma) E = -\frac{i \rho}{\varepsilon_0} K + \omega^2 \mu_0 P_S \qquad (E-36)$$

This relation shows again that it is the polarization in the direction of ${\bf S}$ which is the cause of non-Ohmic

effects. If $P_S = 0$, then E is parallel to K, and no electromagnetic field can exist unless $\rho = 0$ and the dispersion relation becomes independent of the field strength:

$$K^2 = \mu_0 \, \epsilon_0 \, \omega^2 \, \epsilon \, - \, i \, \mu_0 \, \omega \sigma \tag{E-37}$$

This is merely an Ohmic dispersion relation in a medium characterized by a dielectric constant and a conductivity. The dielectric constant differs from unity when $P_{\rm E} \neq 0$. When $P_{\rm S} \neq 0$, the dispersion becomes, from (E-36):

$$K^{2} = \mu_{0} \varepsilon_{0} \omega^{2} \varepsilon - i \mu_{0} \omega \sigma - \frac{\rho^{2}}{\varepsilon_{0}} [\varepsilon_{0} E \cdot E]^{-1}$$
 (E-38)

From (C-17), we have:

$$\Phi_{\rho} = \epsilon_{o} E \cdot E \qquad (E-39)$$

so that the general dispersion relation for a non-Ohmic medium imbedded within an Ohmic medium becomes:

$$K^{2} = \mu_{0} \varepsilon_{0} \omega^{2} \varepsilon - i \mu_{0} \omega \sigma - \frac{\rho}{\Phi \varepsilon_{0}}$$
 (E-40)

Consequently, there will exist potential variations within a non-Ohmic medium, and these potentials will be related to the charge density via a parameter which has the units of capacitance density. That is, the capacitance is defined as the ratio of charge to voltage of a system. The capacitance density is then:

$$\overline{C} = \rho/\Phi$$
 (E-41)

For a parallel plate capacitor, the capacitance can be obtained from Poisson's Law (B-11):

$$EA = \frac{Q}{\epsilon_0 \epsilon} \tag{E-42}$$

so that $C = \frac{Q}{V} = \frac{\varepsilon_0 \varepsilon A}{X}$, where A is the plate area and X the plate separation. The capacitance density is:

$$\overline{C} = \frac{C}{XA} = \frac{\varepsilon_0 \varepsilon}{X^2} \tag{E-43}$$

so that for such a capacitor, the dispersion relation becomes:

$$K^{2} = \mu_{0} \varepsilon_{0} \omega^{2} \varepsilon - i \mu_{0} \omega \sigma - \frac{\varepsilon}{X^{2}}$$
 (E-44)

Thus, the wavevector can be directly varied in a manner proportional to the inverse of the separation between the plates. Equation (E-44) shows that the wavevector in general depends on a capacitative parameter (ε), a conductivity parameter (σ), and a parameter which ultimately depends on the geometrical distribution of interfaces (\overline{C}).

Consequently, non-Ohmic effects due to free charges are embodied in the charge density, as in (E-28), whereas effects due to bound charges are embodied in a capacitance density. For interfacial systems where the charges are largely bound, the non-Ohmic effects appear due to changes in the spacing between the double layers. Thus, the non-Ohmic behavior, whereby interfacial systems can modulate

an impressed electromagnetic field, is associated with a physical change at the interfacial region.



REFERENCES

- 1. K. S. Cole and H. J. Curtis, J. Gen. Physiol. <u>22</u>, 649 (1939).
- D. J. Aidley, <u>The Physiology of Excitable Cells</u>. Cambridge University Press, London (1971).
- 3. A. C. Scott, <u>Neurophysics</u>. John Wiley & Sons, NY (1977).
- 4. J. B. Ranck, Jr., Exp. Neurol. 27, 454 (1970).
- W. R. Adey, R. T. Kado, and J. Didio., Exp. Neurol. 5, 47 (1962).
- 6. A. Van Harreveld and J. P. Schade, Exp. Neurol. <u>5</u>, 383 (1962).
- 7. L. B. Cohen, B. Hille, and R. D. Keynes, J. Physiol. 211, 495 (1970).
- 8. G. N. Berestovskii, et al., Biophysics 15, 60 (1970).
- 9. L. B. Cohen, Physiological Reviews 53, 373 (1973).
- 10. M. H. Sherebrin, et al., Biophys. J. <u>12</u>, 977 (1972).
- 11. H. P. Schwan, Advances in Biological and Medical Physics <u>5</u>, 147 (1957).
- 12. E. C. Burdette, F. L. Cain, and J. Seals, IEEE Transactions on Microwave Theory and Techniques <u>28</u>, 414 (1980).
- 13. B. D. McClees and E. D. Finch, Advances in Biological and Medical Physics 14, 163 (1973).
- 14. S. M. Michaelson, et al., <u>Fundamental Aspects of Non-</u> Ionizing Radiation. Plenum, NY (1975).
- 15. N. H. Steneck, et al., Science 208, 1230 (1980).
- 16. J. B. Gunn, Solid-State Communications 1, 88 (1963).

- 17. T. G. Aaby, Master's Thesis. Michigan State University, Department of Biophysics (1981).
- 18. N. A. Krall and A. W. Trivelpiece, <u>Principles of Plasma Physics</u>. McGraw-Hill, NY (1973).
- 19. B. Oakley and R. Schafer, Experimental Neurobiology. The University of Michigan Press, Ann Arbor (1978).
- 20. R. E. Collin, Field Theory of Guided Waves. McGraw-Hill, NY (1960).
- 21. J. O'M. Bocris and A. K. N. Reddy, Modern Electrochemistry, Vol. 2, Plenum, NY (1970).
- 22. L. G. Abood and W. Hoss, Excitation and Conduction in the Neuron. In G. J. Siegel, et al. (Eds.),

 Basic Neurochemistry, 2nd edition. Little, Brown and Co., Boston (1976).